Icarus 205 (2010) 73–102

Contents lists available at ScienceDirect

Icarus

journal homepage: www.elsevier.com/locate/icarus

Mars Reconnaissance Orbiter observations of light-toned layered deposits and associated fluvial landforms on the plateaus adjacent to Valles Marineris

C.M. Weitz [a,*], R.E. Milliken [b], J.A. Grant [c], A.S. McEwen [d], R.M.E. Williams [a], J.L. Bishop [e], B.J. Thomson [b]

[a] Planetary Science Institute, 1700 E. Fort Lowell, Tucson, AZ 85719, USA
[b] Jet Propulsion Laboratory, Pasadena, CA 91109, USA
[c] National Air and Space Museum, Smithsonian Institution, Washington, DC 20560, USA
[d] Lunar & Planetary Laboratory, University of Arizona, 1541 E. University Blvd, Tucson, AZ 85721, USA
[e] The SETI Institute, 515 N. Whisman Rd., Mountain View, CA 94043, USA

ARTICLE INFO

Article history:
Received 13 November 2008
Revised 20 April 2009
Accepted 21 April 2009
Available online 10 May 2009

Keywords:
Mars
Mars, surface
Mineralogy

ABSTRACT

We have used data from the Mars Reconnaissance Orbiter to study 30–80 m thick light-toned layered deposits on the plateaus adjacent to Valles Marineris at five locations: (1) south of Ius Chasma, (2) south of western Melas Chasma, (3) south of western Candor Chasma, (4) west of Juventae Chasma, and (5) west of Ganges Chasma. The beds within these deposits have unique variations in brightness, color, mineralogy, and erosional properties that are not typically observed in light-toned layered deposits within Valles Marineris or many other equatorial areas on Mars. Reflectance spectra indicate these deposits contain opaline silica and Fe-sulfates, consistent with low-temperature, acidic aqueous alteration of basaltic materials. We have found valley or channel systems associated with the layered deposits at all five locations, and the volcanic plains adjacent to Juventae, Ius, and Ganges exhibit inverted channels composed of light-toned beds. Valleys, channels, and light-toned layering along the walls of Juventae and Melas Chasmata are most likely coeval to the aqueous activity that affected the adjacent plateaus and indicate some hydrological activity occurred after formation of the chasmata. Although the source of water and sediment remains uncertain, the strong correlation between fluvial landforms and light-toned layered deposits argues for sustained precipitation, surface runoff, and fluvial deposition occurring during the Hesperian on the plateaus adjacent to Valles Marineris and along portions of chasmata walls.

1. Introduction

Light-toned layered deposits (LLDs) have been targeted by the Mars Reconnaissance Orbiter (MRO) in several locations along the Hesperian-aged volcanic plains adjacent to Valles Marineris, including (1) south of Ius Chasma, (2) southwest of Melas Chasma, (3) south of western Candor Chasma, (4) northwest of Juventae Chasma, and (5) west of Ganges Chasma (Fig. 1). These light-toned layered deposits on the plateaus adjacent to Valles Marineris (VM plateau LLDs) are only seen in locations where there has been erosion of an unconformably overlying meters-thick darker-toned unit or along crater and trough walls, although the LLDs could be more areally extensive than seen by these exposures. Additional smaller outcrops of LLDs may exist outside of these five locations, but they have not yet been identified. Originally observed in Mars Orbiter Camera (MOC) images (Edgett, 2005; Edgett and Malin, 2003, 2004), the VM plateau LLDs were interpreted as deposits with similar properties to the units at Sinus Meridiani. They occur at or above volcanic plains mapped to be Early Hesperian in age (McCauley, 1978; Whitbeck et al., 1991; Scott and Tanaka, 1986). Mantling most of the LLDs is a darker-toned material that is most likely eolian debris but could contain a component of impact regolith. While several other locations along the plateaus have light-toned surfaces, the VM plateaus LLDs consist of multiple finely-stratified beds, indicating they are sedimentary strata rather than a surface coating or an individual layer of light-toned material.

Light-toned layered deposits, including the Interior Layered Deposits (ILDs) found in Valles Marineris, occur in many locations on Mars (e.g., Malin and Edgett, 2000), suggesting the processes responsible for their emplacement were widespread in the martian past. There are many hypotheses for the origin of the ILDs in Valles Marineris: (1) lacustrine sedimentary deposition (McCauley, 1978; Spencer and Croft, 1986; Nedell et al., 1987; Spencer and Fanale, 1990; Komatsu et al., 1993; Malin and Edgett, 2000, 2001); (2) volcanic deposition (Peterson, 1982; Lucchitta, 1990; Lucchitta et al., 1994; Chapman and Tanaka, 2001; Hynek et al., 2003); (3) mass wasting of material from the chasmata walls (Nedell et al., 1987; Lucchitta et al., 1994); and (4) aeolian/airfall deposition (Peterson,

* Corresponding author. Address: Planetary Science Institute, 1700 E. Fort Lowell, Suite 106, Tucson, AZ 85719, USA.
E-mail address: weitz@psi.edu (C.M. Weitz).

0019-1035/$ - see front matter © 2009 Elsevier Inc. All rights reserved.
doi:10.1016/j.icarus.2009.04.017

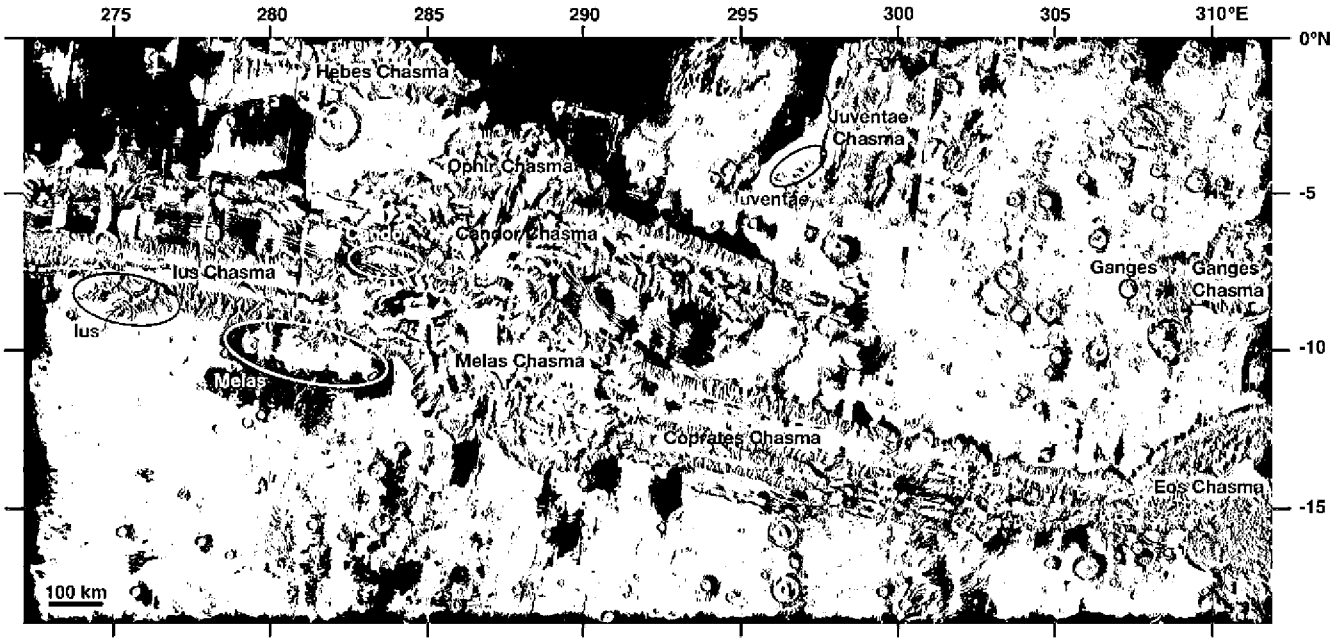

Fig. 1. Map of Valles Marineris showing the five locations where light-toned layering and valleys were analyzed along the plateaus. THEMIS daytime infrared mosaic.

1982; Nedell et al., 1987; Malin and Edgett, 2000; Catling et al., 2006). Recent results using MRO data for the ILDs in western Candor Chasma indicate that the light-toned layered sediments post-date formation of the chasma (Okubo et al., 2009) and are composed of lithified eolian material mixed with crystalline hematite, monohydrated sulfates, and polyhydrated sulfates (Murchie et al., 2009). In addition, the ILD in eastern Candor Chasma contains alternating layers of monohydrated and polyhydrated sulfates (Roach et al., 2009).

The ILDs within Valles Marineris and the LLDs on the plateaus differ in lithology from the dark-toned layered strata that form much of the wallrock in Valles Marineris. The wallrock is apparently variable in strength and cohesion, but consist of competent layers, perhaps lava flows, interbedded with thicker stacks of weaker layers that may be volcanic ash or other sedimentary deposits (Beyer and McEwen, 2005). The dark layers that compose the wallrock have previously been interpreted as volcanic lavas (McEwen et al., 1999), sedimentary rocks (Malin and Edgett, 2001), and/or layered intrusives (Williams et al., 2003). A dark-toned unit also exists on the adjacent plateaus and covers much of the LLDs in this region. Unlike the dark-toned units in the wallrock, ripples are commonly found within this dark mantle, indicating past or current mobility of eolian material.

The VM plateau LLDs show complex stratigraphic sequences where individual beds can be distinguished based upon variations in their color, brightness, compositional, and erosional style (Weitz et al., 2008; Le Deit et al., 2008a). Alternating dark and light banding is a characteristic of many of the ILDs but high-resolution images from MOC and HiRISE suggest that the dark bands represent terrain where dark debris has accumulated rather than a physical property of the beds (Malin and Edgett, 2000; Weitz et al., 2007). The MRO Compact Reconnaissance Imaging Spectrometer for Mars (CRISM) spectra reveal that the composition of the VM plateau LLDs is distinct from the ILDs. The former contain opal (hydrated silica) and Fe-sulfates, phases that are consistent with alteration of basaltic materials (Milliken et al., 2008), whereas the ILDs contain monohydrated and polyhydrated sulfates (Murchie et al., 2009; Bishop et al., 2009; Roach et al., 2009). The geomorphic and mineralogic differences between the ILDs and LLDs imply depositional or alteration processes on the VM plateaus that are distinct from those within the troughs (Weitz et al., 2008). Although ILDs within Valles Marineris chasmata have been extensively studied for several decades, limited analyses (e.g., Edgett, 2005) have been conducted prior to MRO on the VM plateau LLDs that are discussed in this paper.

Carr (1995) found that martian valley networks observed in Viking images are primarily located on cratered uplands in the southern hemisphere of Mars at surface elevations >2 km. Ninety percent of the networks occur in Noachian-aged terrain, with the youngest valley networks found only on volcanoes. The drainage density for most valleys on Mars falls between 10^{-2} and 10^{-1} km/km^2 on dissected surfaces, which is one to three orders of magnitude less than typical terrestrial values (Grant, 1987; Cabrol and Grin, 2001; Gulick, 2001; Irwin and Howard, 2002; Craddock and Howard, 2002). In stark contrast to these general statements, however, dendritic valleys occur within and along Valles Marineris and possess densities exceeding 1.0 km^{-1} (Mangold et al., 2004; Williams et al., 2005; Mangold et al., 2008). These dendritic valleys discovered prior to MRO are found on the plateau west of Echus Chasma, on the plateau adjacent to Juventae Chasma, and along the wallrock of a basin in southwestern Melas Chasma. Mapping of the Melas valley networks by Quantin et al. (2005) suggested these valleys were incised by runoff from a lengthy period of precipitation that may have extended well into the Hesperian. The fine-bedded LLDs on the plateaus adjacent to Juventae and Ganges Chasmata have associated valleys and inverted channels (Weitz et al., 2008). Our targeting and analyses of High Resolution Imaging Science Experiment (HiRISE) images has revealed additional valley networks in association with the LLDs and we discuss these valleys as well and their support for a fluvial origin of the VM plateau LLDs.

2. Data sets

We have analyzed recent MRO data from the HiRISE camera (McEwen and 14 colleagues, 2007; McEwen and 69 colleagues, 2009), Context Camera (CTX) (Malin et al., 2007), and CRISM (Murchie et al., 2007). The ability to characterize the VM plateau LLDs has been greatly aided by HiRISE. The high resolution (25–60 cm/pixel) of these images enables observations of very small exposures of light-toned strata beneath the dark-toned surficial mantle. Color HiRISE images exhibit variations likely linked to differences

in composition not observable by previous monochromatic cameras, and stereo image pairs provide valuable information about stratigraphic relationships within the deposits and to adjacent units. CRISM visible and near-infrared spectra of the VM plateau LLDs were also examined to identify compositional variations within the LLDs, providing insight into the aqueous alteration and possible origin of these units (Milliken et al., 2008). Finally, the CTX images (spatial scales of 6 m/pixel) permit a regional view of the VM plateau LLDs and neighboring terrain, thereby providing context and helping to identify or infer additional occurrences of LLDs and other geologic units where HiRISE images have not yet been acquired. Together, the synthesis of these three datasets provides valuable morphologic and mineralogic information needed to interpret the geologic setting and origin of the VM plateau LLDs that was unobtainable prior to the MRO mission.

All HiRISE images used in this study are NOMAP products, meaning they have not been geometrically projected to north at the top of the image (McEwen and 69 colleagues, 2009). Instead, all of the HiRISE images in this paper have north approximately 7° to the right of top unless otherwise noted. HiRISE false-color images were made by displaying the IR, RED, and BG channels in red, green, and blue, respectively (McEwen and 14 colleagues, 2007, 2009). For color images, each color band is individually stretched to maximize contrast, so the colors are enhanced differently for each image based on the color and brightness of each scene. HiRISE stereo anaglyphs are produced by displaying the more left-looking image (smaller or more negative roll angle) in red and the more right-looking in both green and blue (McEwen and 69 colleagues, 2009). When viewed with red-blue glasses, the image appears as an anaglyph showing a three-dimensional view. We did not attempt to extract albedos from the VM plateau LLDs because of complexities associated with removing both atmospheric scattering and contamination by surficial eolian debris.

CTX images were mosaicked manually using the software program Adobe Photoshop so there are geometric errors in the mosaics, most notably along the walls and floors of the chasmata. For this investigation, however, we are only interested in the deposits along the plateau where there are very small or no errors in geometry in the CTX mosaics that we used for mapping. All CTX images are oriented with north at the top.

CRISM radiance data were divided by the solar input and photometrically corrected by dividing by the cosine of the solar incidence angle, resulting in I/F spectra (Murchie et al., 2007; Mustard et al., 2008). Contributions from atmospheric components were minimized by dividing each spectrum by a scaled atmospheric transmission spectrum derived from observations over Olympus Mons (Mustard et al., 2008). The data were also corrected using an in-scene flat field correction to reduce noise, in which each pixel was multiplied by the ratio of the scene to detector column average. Finally, the band parameters of Pelkey et al. (2007) were calculated for each CRISM image and all images were map-projected. The data have been corrected for atmospheric gases but not aerosols, and therefore they are not true surface reflectance. All spectra presented here are CRISM I/F ratio spectra. These ratio spectra were created by averaging pixels (typically 100–600 pixels) corresponding to distinct geologic or lithologic units and dividing the result by an average of pixels from a spectrally 'unremarkable' region, usually corresponding to the ubiquitous Mars dust (Mustard et al., 2008; Milliken et al., 2008). The resulting spectrum enhances the features of interest (usually hydration features) relative to those seen in dusty regions. All CRISM RGB images (where Red = ~2.5 μm, Green = ~2.1 μm, Blue = ~1.1 μm) use the same bands and wavelengths.

3. Ius plateau

3.1. Ius plateau LLD

Ius Chasma extends from Noctis Labyrinthus to the west and Melas Chasma to the east. Along the southern wall are branching

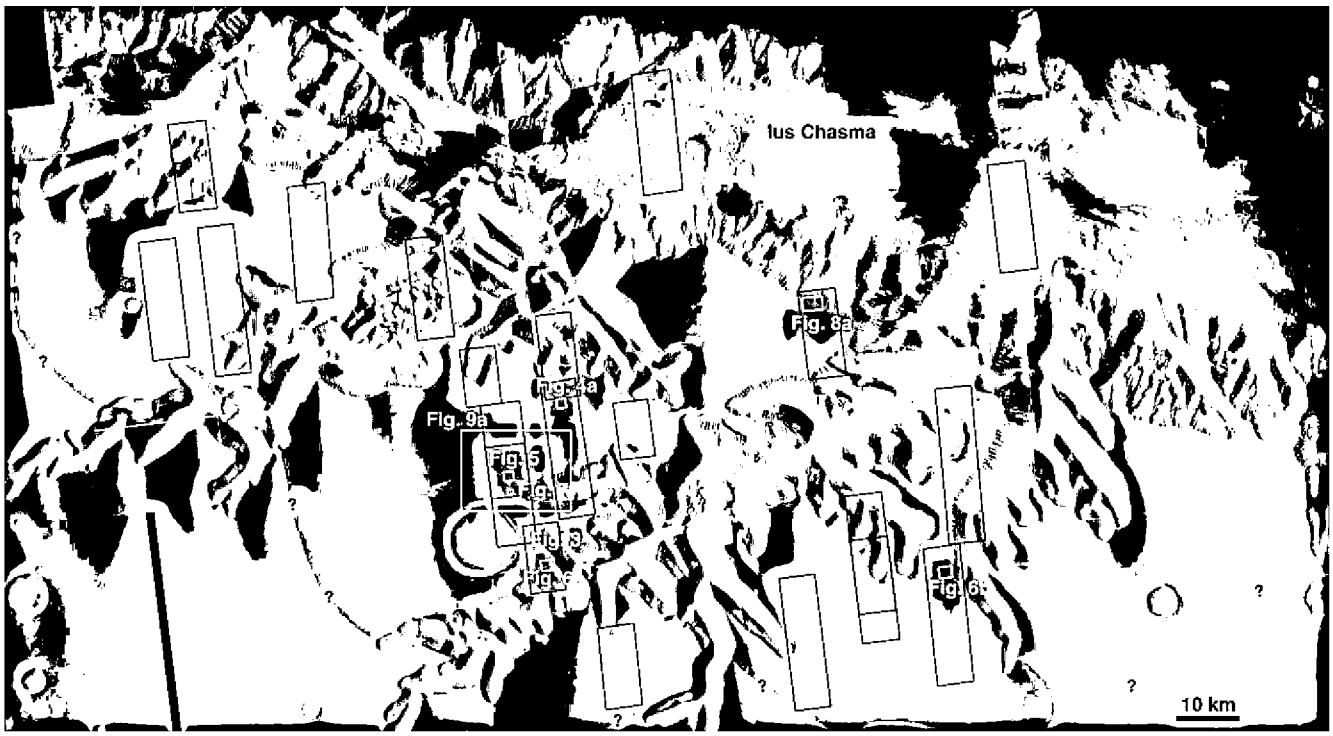

Fig. 2. CTX mosaic of the plateau south of Ius Chasma where we have mapped the LLD in purple and likely LLD in brown. Black rectangles identify HiRISE images that have been acquired. Yellow boxes identify later figures. Illumination direction is from the left. (For interpretation of color mentioned in this figure the reader is referred to the web version of the article.)

Fig. 3. Portion of HiRISE image PSP_3804_1715 showing color heterogeneities along individual beds, as well as between beds, in the LLD. Illumination is from the lower left. (For interpretation of color mentioned in this figure the reader is referred to the web version of the article.)

tributary canyons thought to have formed by groundwater sapping (Kochel and Piper, 1986; Lucchitta and 9 colleagues, 1992), and it is along the longest and most prominent of these tributary canyons (Louros Valles) that the LLD is best exposed (Fig. 2). Although we distinguish the Melas and Ius plateau deposits as distinct units, it is possible they are actually one single areally extensive unit buried beneath a dark-toned mantle that prevents us from confidently joining them together.

A pair of HiRISE images with one taken at the beginning of the 2007 global dust storm (PSP_4648_1720) and the same area re-imaged after the dust storm (PSP_6850_1720) shows numerous dark wind streaks in the later image that were not seen a few weeks earlier, suggesting dust was deposited on the surface during the storm and then subsequently modified by winds. The deposition of dust during this storm, as well as prior dust storms, may obscure thinner exposures of the LLD and prevent the full extent of the deposit from being mapped. Additionally, the dust may hinder our ability to detect mineralogic signatures indicative of LLDs in the CRISM data.

In any given group of strata, we can distinguish different beds based upon brightness and color variations (Fig. 3). In some instances the dark-toned layers may result from surficial cover by relatively darker eolian debris. However, in cases where the layer brightness is homogeneous across topographic and spatial distances, and the contact between a bright and darker layer has a sharp rather than diffuse edge, the dark-toned nature can be attributed to properties of the bed itself rather than surficial debris. Color differences seen in HiRISE images also appear to reflect physical or compositional variations rather than surficial contamination. Individual beds can also show heterogeneities in color (Fig. 3) that could reflect mixtures of materials in the sediments that compose

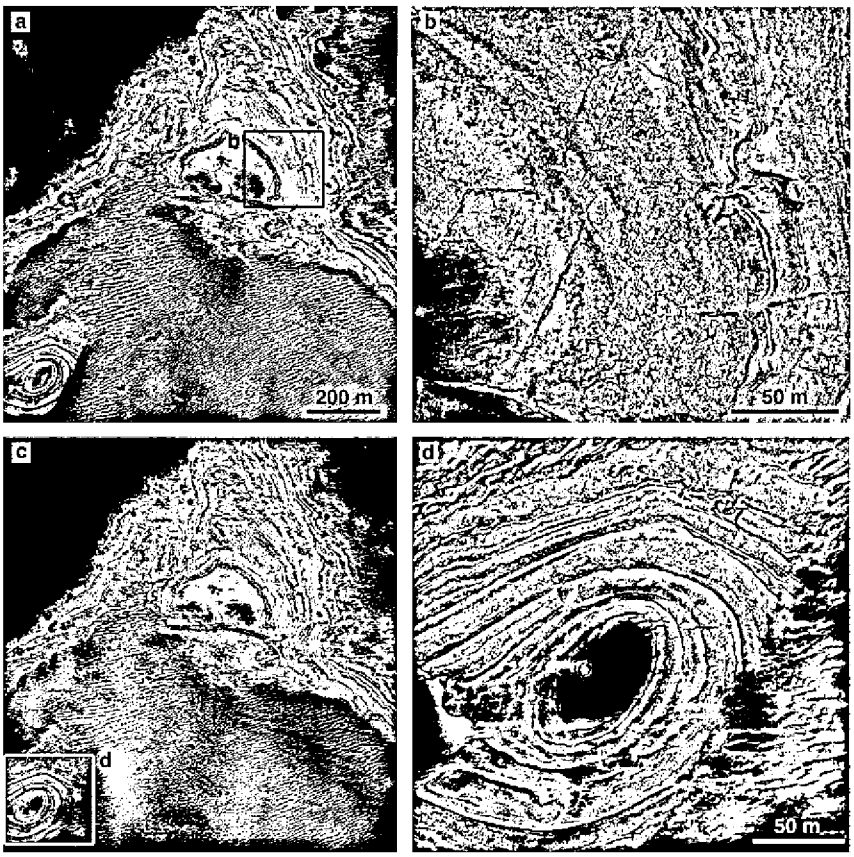

Fig. 4. (a) Example of strata in the Ius plateau. A brown rippled surficial mantle (bottom) and a black debris mantle (upper left) cover much of the LLD. Red box shows location of blowup in (b) where polygonal fractures and color variations are visible in the beds. Portion of HiRISE false-color image PSP_2459_1715. Illumination is from the upper left. (c) Stereo anaglyph of the same region shown in (a). Location of blowup shown by yellow rectangle. Portion of HiRISE images PSP_2459_1715 and PSP_3092_1715. (d) Bench-cliff erosional morphology is evident in the stereo anaglyph blowup. A dark-toned eolian mantle covers the uppermost surface of the LLD as well as lower-lying strata (lower right). (For interpretation of color mentioned in this figure the reader is referred to the web version of the article.)

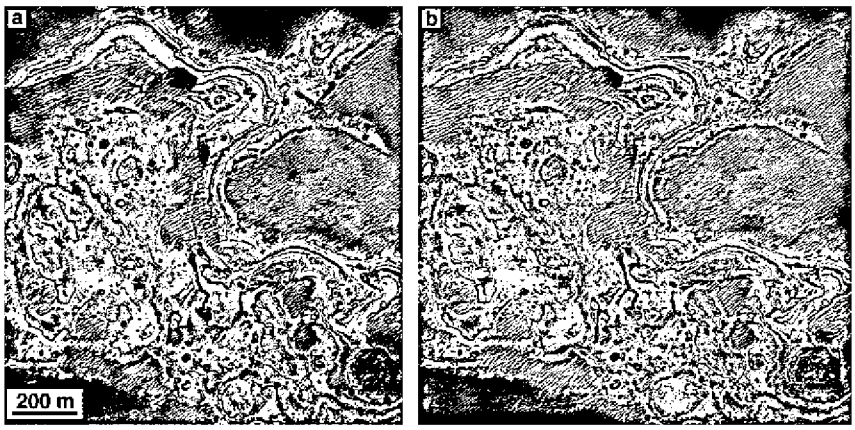

Fig. 5. (a) False-color image of the Ius plateau LLD. Polygonal fracturing can be seen in broader exposures of light-toned beds that correspond to opaline silica. The black circles are eroded impact craters that have been partially filled by dark-toned eolian debris. Illumination is from the lower left. (b) Stereo anaglyph showing the same area in (a). Hills and undulations are apparent along the uppermost surfaces of both the light-toned and dark-toned beds. Eolian ripples cover all stratigraphic levels. Portion of HiRISE images PSP_5149_1715 and PSP_5215_1715. (For interpretation of color mentioned in this figure the reader is referred to the web version of the article.)

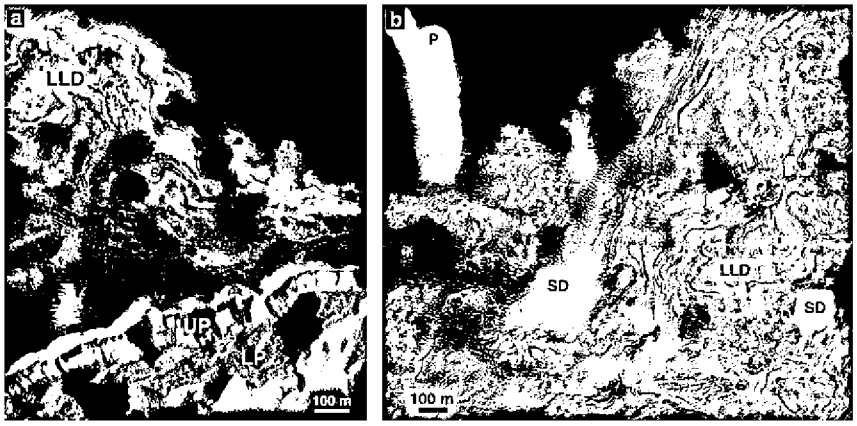

Fig. 6. Examples of the stratigraphy along the Ius plateau LLD. (a) The LLD is above the volcanic plains units, which can be seen along a tributary canyon. We have divided the lava plains into two units: a lower plains (LP) that appears rough and has pronounced bedding, and an upper plains (UP) which appears smoother with limited bedding. Portion of HiRISE false-color image PSP_3804_1715. Illumination is from the lower left. (b) Stereo anaglyph that shows surficial debris (SD) covers much of the LLD. A lava plains unit (P) is stratigraphically below the LLD and it too is mantled by surficial debris. Portion of HiRISE images PSP_7786_1710 and PSP_9935_1710.

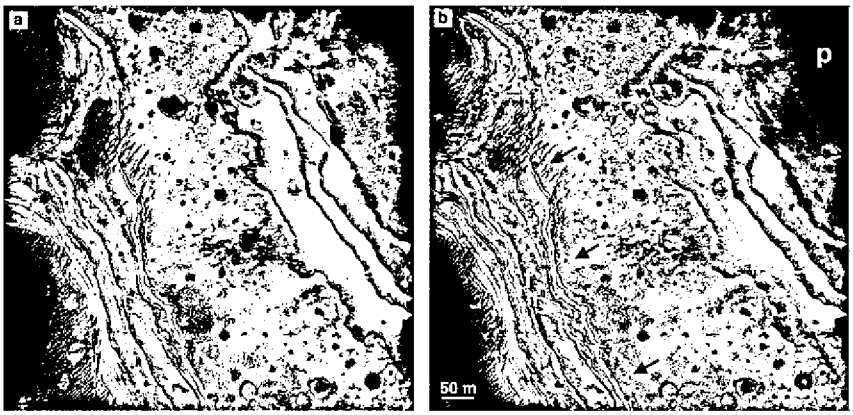

Fig. 7. Geologic contacts between different beds in the LLD. (a) Portion of HiRISE RGB image PSP_5215_1715 of light-toned and dark-toned beds in the strata. Illumination is from the lower left. (b) Stereo anaglyph of the same region shown in (a). Several of the light-toned beds appear finely layered with small exposures along their surfaces (*f*). A light-toned bed with a large exposure along its surface (*t*) has numerous old impact craters (black circles) and polygonal fractures. CRISM data indicate an opaline silica composition for this bed. The geologic contact between units *f* and *t* is shown by the black arrows. The lowermost beds in the LLD strata are dark-toned but morphologically distinct from the rougher lava plains unit (*p*) that lies below them. Portion of HiRISE images PSP_5215_1715 and PSP_5149_1715. (For interpretation of color mentioned in this figure the reader is referred to the web version of the article.)

the beds or post-deposition alteration of the beds, such as chemical weathering. Alternatively, these multicolored beds may be composed of multiple beds that are too thin to be individually resolved by HiRISE.

The surfaces of individual light-toned beds are commonly characterized by polygonal fractures (Le Deit et al., 2008b) that are variable in size (1–10 m in diameter) and shape between and within layers (Fig. 4). The polygons could have formed by thermal contraction or through dessication of hydrated materials and are commonly seen on other LLDs elsewhere on Mars (e.g., Mawrth Vallis; Wray et al., 2008). In several locations, the fractures appear to be the result of cracking and erosion of an individual layer. The polygonal fractures are a diagnostic characteristic of the LLDs that can be found on the majority of light-toned beds. Consequently, we have used the identification of polygonal fractures on light-toned material when mapping the LLDs, particularly in small exposures where only a few light-toned beds are visible.

As noted by Weitz et al. (2008), the VM plateaus LLDs display a stair-step pattern in the strata resulting from differential erosion that creates flatter benches and steeper cliffs (Fig. 4). This cliff-bench pattern and the thickness of beds appear to be irregular, unlike LLDs found inside craters in Arabia Terra (e.g., Becquerel) where the layers appear to be of similar composition and thickness such that the cliff-bench pattern is repetitive and rhythmic (Lewis et al., 2008). The observation that some layers have broad flat upper capping surfaces whereas others erode more easily and have little or no horizontal exposures likely results from differences in the material properties and/or particle sizes of the materials that compose the layers. The color variations and distinct style of polygonal fractures seen in different layers also supports the presence of compositional variation in the strata. Either the sediments or degree of cementation changed over time, or only some layers experienced post-depositional alteration that caused them to become more or less friable relative to other layers.

Observations from stereo HiRISE images suggest the surface of the LLD is not always smooth and flat but instead can sometimes display slight topographic variations (Fig. 5), perhaps due to differential erosion as the topmost layer is preferentially removed, presumably by wind. MOLA profiles across the Ius plateau LLD indicate total thicknesses on the order of 30 m. We have identified between 20 and 30 beds in some of the thicker sections. For a sequence thickness of 30 m, this would imply that individual beds are on the order of ~1 m thick. We have not yet observed any clear evidence of cross-bedding in any of the VM plateaus LLD outcrops discussed here, either because it does not exist or it is at a scale below the resolution of HiRISE images.

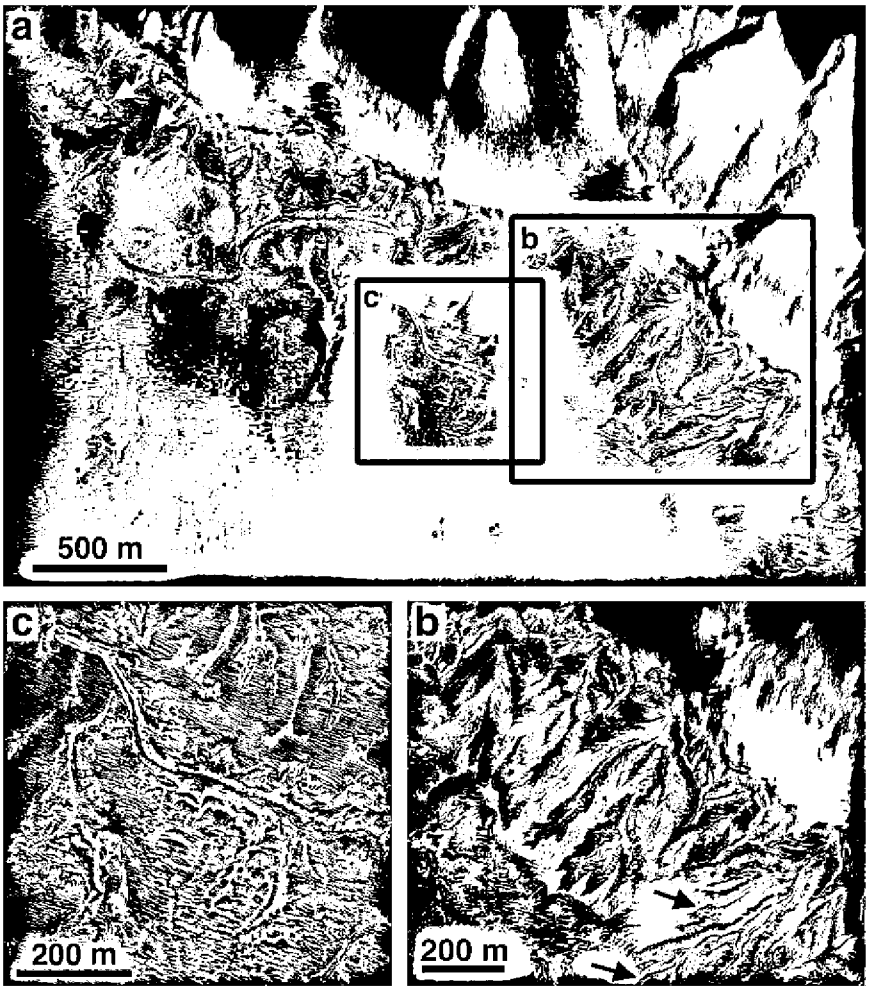

Fig. 8. (a) Valleys in the Ius plateau LLD. The valleys have thus far only been seen along this northern portion of the LLD next to Ius Chasma. Yellow arrows indicate flow direction. Blowups in (b) and (c) are shown by black boxes. Portion of HiRISE image PSP_010423_1720. Illumination is from the left. (b) False-color image with possible inverted channels identified by black arrows. (c) Blowup of possible eroded depositional fan. (For interpretation of color mentioned in this figure the reader is referred to the web version of the article.)

The Ius LLD lies stratigraphically above the Hesperian volcanic plains, and in many locations we have identified an upper plains and a lower plains unit that differ in their lithology (Fig. 6a), similar to units discussed by Milliken et al. (2008). The upper plains unit appears smooth with small discontinuous outcrops of layers. In contrast, the lower plains unit is rough with many exposed layers and sharp spurs. The LLD appears to have been eroded back several tens of meters from the edges of the Ius tributary canyons, suggesting the deposit is more friable than the underlying plains. The LLD, especially adjacent to tributary canyons, stands topographically above the plains (Fig. 6b). HiRISE stereo pairs of the LLD allow us to determine that the bedding appears to be parallel and approximately horizontal within any given stereo image, with uneven surfaces on the uppermost beds likely due to wind erosion.

Fig. 7 shows the geologic contact between a stratigraphically underlying light-toned polygonally fractured bed, *t*, and upper finer-layered beds, *f*. CRISM data indicate that the light-toned bed (*t*) contains opaline silica, whereas the fine-layered beds lack diagnostic spectral features (Milliken et al., 2008). Stratigraphically beneath bed *t* are at least three dark-toned beds with the volcanic plains unit, *p*, at their base. Although bed *t* is stratigraphically beneath the beds in *f*, the HiRISE stereo pairs reveal that bed *t* can sometimes be topographically above several of the beds in *f*. One way to produce this geologic arrangement is to have differential erosion of bed *t* that created localized topographic lows that were subsequently filled with the finer beds (*f*). Higher standing portions of bed *t*, like those seen in this figure, are not obscured by the finer-layered beds. These stratigraphic relationships and differences in morphology suggest that variable depositional processes and/or deposition of different materials may have occurred in distinct time periods. The lower thicker beds (*t*) were deposited first, followed by differential erosion and then deposition of the thinner

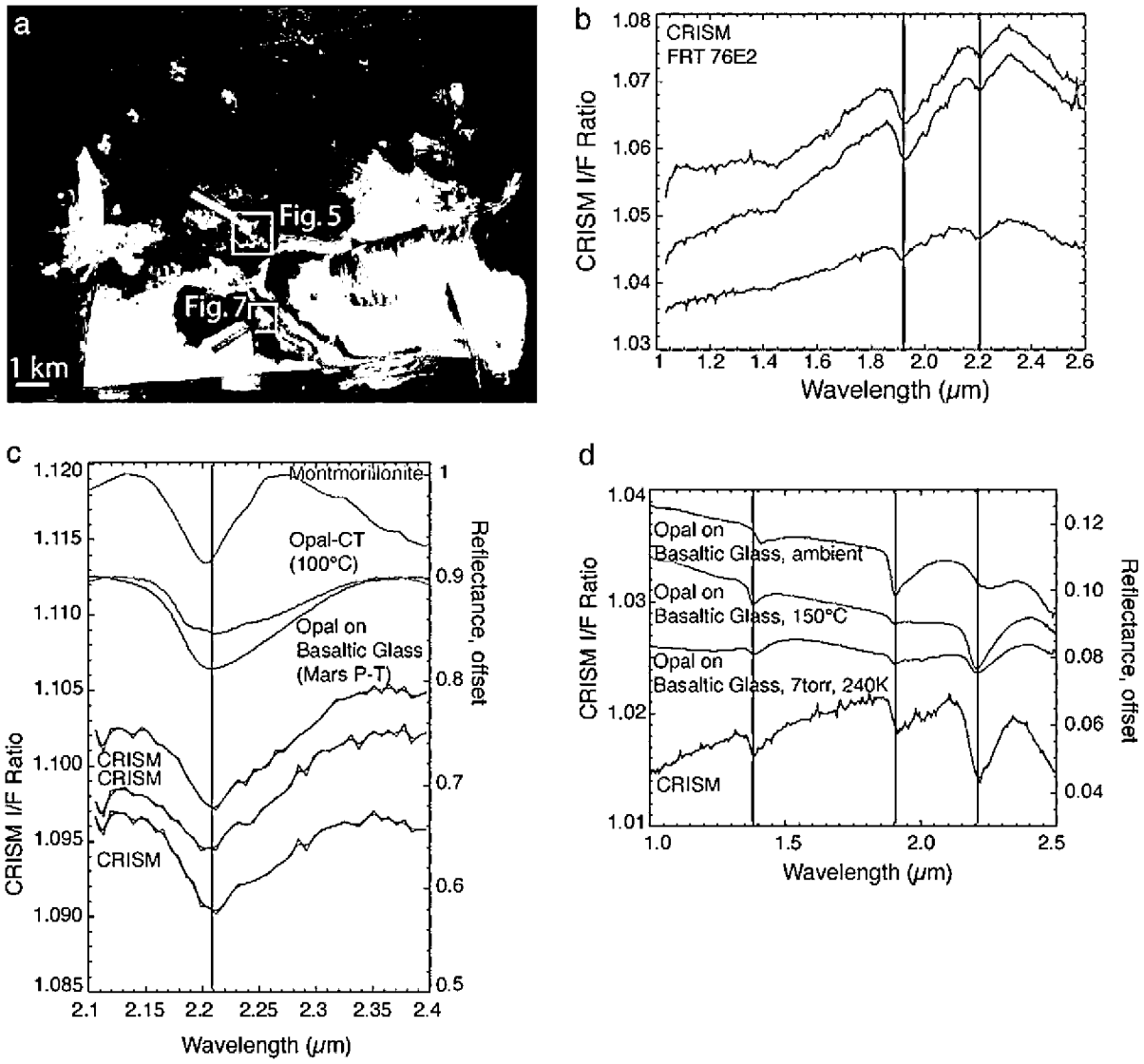

Fig. 9. (a) CRISM false-color RGB image (FRT 76E2) overlaid on a CTX mosaic. The bluish and whitish colors correspond to outcrops of LLD. The colored arrows correspond to locations of the spectral ratios in (b). White boxes shows the location of HiRISE blowups in Figs. 5 and 7. Illumination is from the left. (b) CRISM ratio spectra corresponding to locations shown by arrows in (a). These spectra are most consistent with opaline silica. (c) Laboratory spectra for montmorillonite, opal-CT, and opal coated basaltic compared to CRISM ratio spectra. The band center, width, and asymmetry of the CRISM bands are more consistent with opal than a clay mineral such as montmorillonite. The opal-CT was partially dehydrated by heating and is similar to opal that has been dehydrated by measuring it under Mars-like pressure and temperature conditions (Milliken et al., 2008). (d) Comparison of laboratory spectra of opal under various conditions to a CRISM ratio spectrum acquired near Ius Chasma. The shift of the 1.41 μm band to 1.38 μm is observed in the CRISM data and is most consistent with opal that has lost some H_2O. This band shift is not observed in clays or unaltered hydrated glass. (For interpretation of color mentioned in this figure the reader is referred to the web version of the article.)

but more numerous upper beds (*f*). Bed *t* and the underlying dark-toned beds are only observed adjacent to the tributary canyons, either because these are the best and deepest exposures of these underlying units or because they were only deposited in these locations. It cannot be ascertained if the underlying beds are darker because they are covered with dark surface debris or if the beds themselves are actually lower in albedo. The color and brightness of these dark-toned beds is consistent with those of the surficial mantle observed throughout this region. However, the surficial mantle is generally composed of ripples and their absence on the bed surfaces would argue against eolian debris as the cause of their darker-toned nature.

3.2. Ius plateau fluvial landforms

Only one HiRISE image (PSP_010423_1720) thus far shows fluvial landforms associated with the LLD along the Ius plateau, although CTX images indicate additional valleys to the west of this HiRISE image. The branching landforms located in the north portion of the LLD adjacent to the rim of Ius Chasma (Fig. 8) have a planimetric pattern similar to terrestrial fluvial networks. Many of these inferred fluvial landforms are dense and space-filling, with third order or higher networks. The subtle relief for these fluvial landforms supports atmospheric precipitation as the fluid source. At this location, erosion has penetrated multiple stratigraphic levels revealing different time horizons in a very small geographic area. Further complicating interpretation of this region are eolian debris fill, including ripples, and variations in morphology of the exhumed landforms. Within 100 m of the chasma rim there are valleys, some of which form branching networks. Typically, these valleys contain relatively bright materials. Further south from the chasma are branching networks that apparently have subtle to no relief and are marked by alternating concentric medium- and dark-toned materials, some of which may be eolian fill. Although most of these features are negative in relief, a few appear to be inverted (Fig. 8b).

Inferred flow direction can be determined from the fluvial landforms based on segment junctions that typically point in the downslope direction (i.e. the segments that form an acute angle are located upslope from the confluence segment). The direction of former water flow derived from this technique is variable and often counters the gentle regional slope (~0.003°) downward to the north obtained from MOLA profiles. The negative relief valleys near the chasma rim appear to have a drainage direction towards the south (away from Ius Chasma) whereas other fluvial landforms indicate a flow towards or parallel to the chasma edge. These different flow directions, as well as the distinct valley morphologies and infilling, could result from separate episodes of surface flow during the Hesperian. We infer the sometimes contrary flow directions as a record of small scale changes in local slope presumably due to eolian deposition over time rather than the presence of drainage divides, although tectonic tilting could have also caused changes in flow direction with time. In addition, the close proximity of apparently contradictory paleoflow directions raises the possibility that some of the landforms are depositional forms (e.g., distributary fans) (Fig. 8c), which bear a resemblance to those seen in the Melas Chasma basin (Quantin et al., 2005; Williams et al., 2005; Metz et al., 2009). In shallow relief settings, streams can transition from a convergent to a divergent network.

The bedrock just below these fluvial landforms is exposed along the upper chasma edge and exhibits no clear evidence of modification by water, indicating the fluvial activity was either confined to the plateau or that more recent mass wasting has destroyed any fluvial landforms that may have been present in the wallrock. Because we have not identified fluvial landforms in any other HiRISE images across the Ius plateau LLD, even where there are large exposures of strata, it is possible that surface flow may have only occurred along the plateau directly adjacent to Ius Chasma.

3.3. CRISM results for the Ius plateau LLD

Several CRISM Full Resolution Targeted (FRTs; ~18 m/pixel), Half Resolution Long observations (HRLs; ~36 m/pixel), and Half Resolution Short observations (HRSs; ~36 m/pixel) acquired along the plateau south of Ius were examined to determine the mineralogy of the LLDs. As visible in Fig. 9a, the LLDs often exhibit bluish or greenish colors in CRISM false-color images. Previous work by Milliken et al. (2008) has shown that some of the light-toned strata exhibit spectral signatures consistent with the presence of opaline silica ($SiO_2 \cdot nH_2O$). In this region, the opal-bearing beds are brighter than the surrounding lava plains material and slightly brighter than bluish non-opaline beds in the LLD (Fig. 9a). The opaline silica signatures (Fig. 9b) are strongest in regions that have been eroded along bedding planes and that exhibit polygonal fractures (Figs. 5 and 7), but it is also clear that not all light-toned beds exhibit spectral evidence for hydrated phases. In particular, many of the bluish beds in the LLD lack diagnostic absorption features and, with the exception of their brightness, are spectrally similar to the mantle material on the surrounding lava plains.

Opaline silica can be distinguished from clay minerals and hydrated glass based on the center position, width, and symmetry of the Si–OH absorption near ~2.21 μm (Milliken et al., 2008). Opal commonly exhibits two overlapping bands near ~2.21–2.26 μm, whereas hydrated glass and clay minerals such as montmorillonite commonly exhibit a single, more symmetrical absorption centered at ~2.22–2.23 μm and ~2.2 μm, respectively (Fig. 9c). Under Mars-like pressure and temperature conditions, H_2O is detached from the SiOH groups and the strongest OH^- overtone absorption near ~1.41 μm shifts to ~1.38 μm (Fig. 9d). A similar effect is not observed for hydrated glass and clays under low relative humidity (Milliken and Mustard, 2005; Milliken et al., 2008). Therefore, a relatively wide absorption band with a minimum at ~2.21 μm, a possible shoulder near ~2.25–2.26 μm or asymmetry at the long wavelength edge of this band, and the presence of an OH absorption at ~1.38 instead of ~1.41 μm are criteria that can be used to distinguish opaline silica from hydrated glass and Al-rich clay minerals (Goryniuk et al., 2004; Milliken et al., 2008). The CRISM data show that at least some of the beds in the LLD near Ius Chasma contain opaline silica, but spectra for the majority of the exposed strata here lack features indicative of hydrated minerals.

4. Melas plateau

4.1. Melas plateau LLD

This region was obscured by atmospheric dust during the 2007 dust storm event, causing much of the surface to be covered beneath a thin veneer of dust after the storm subsided. Dark wind streaks are also commonly seen in HiRISE images acquired after the dust storm. We have used THEMIS (Thermal Emission Imaging System) nighttime infrared images to target HiRISE images where the best exposures of LLD occur along a thermally cool–warm boundary and very close to the canyon edge (Fig. 10). The cooler terrain in the nighttime IR data can be attributed to eolian bedforms that cover most surfaces but are not observed to the south where the THEMIS nighttime images appear warmer. We can identify exposures of LLD on all edges of the deposit and have mapped the LLD between these outcrops with the assumption that it underlies the eolian materials even though there are no surface exposures of light-toned layering. The best exposures

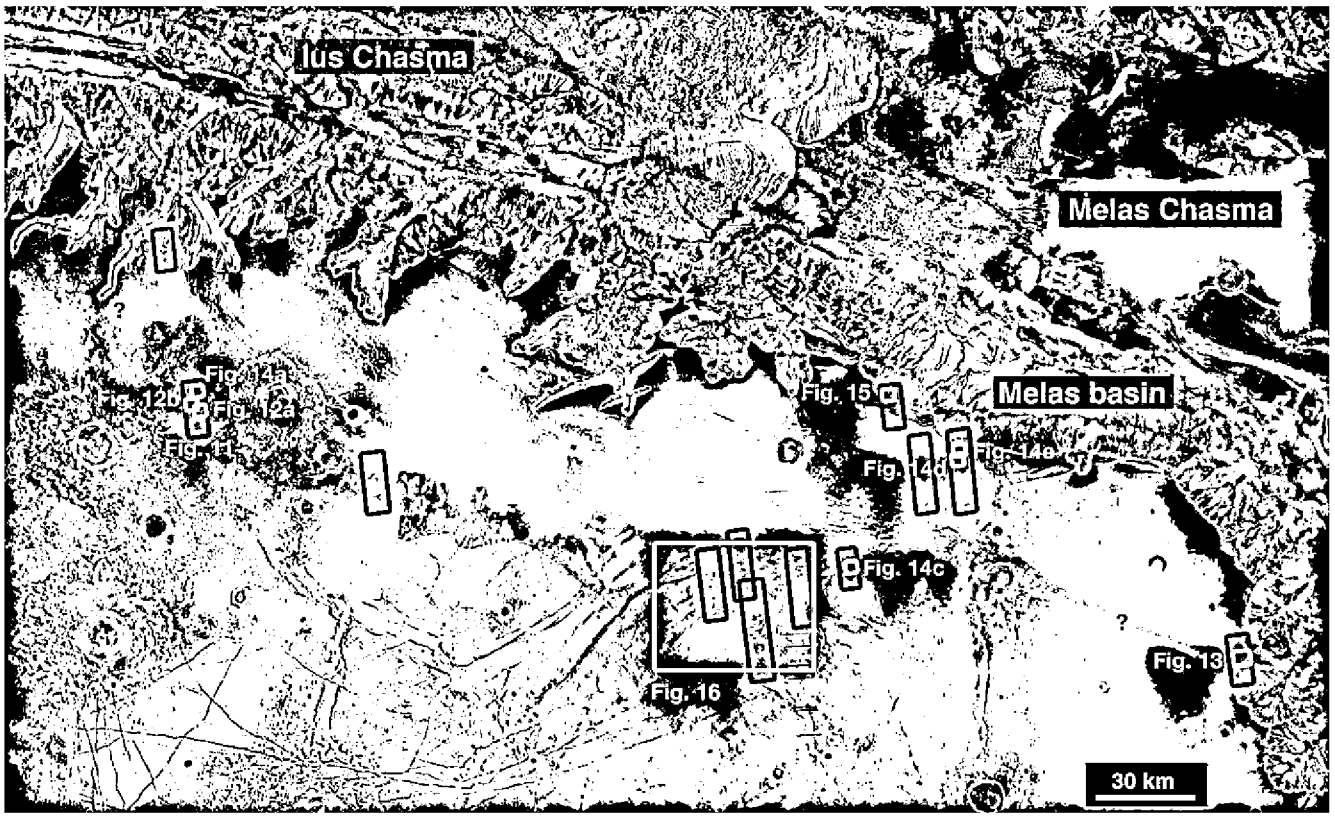

Fig. 10. THEMIS nighttime infrared mosaic of the plateau southwest of Melas Chasma. The LLD is mapped in purple. Black boxes mark locations of current HiRISE images and yellow boxes indicate locations of later figures. The best exposures of the LLD occur along the boundary between the cooler and warmer terrains in the THEMIS image. Valleys and layered deposits are seen both along the plateau and in the Melas basin. (For interpretation of color mentioned in this figure the reader is referred to the web version of the article.)

of light-toned beds along the eastern margin are observed along a narrow (~1 km wide) exposure that parallels the Melas Chasma edge.

The morphology of these strata is similar to the Ius plateau LLD (Fig. 11). There are variations in color both between and within beds. The light-toned beds do not display as much polygonal fracturing, however, and there are ridges in some beds that could result from compression or fracture fill (Fig. 12a). Surfaces of the dark mantles can exhibit circular pitting (Fig. 12b). The pitting is most prevalent in HiRISE images surrounding a fresh 9.7 km diameter impact crater centered at −9.8° and 279.4°E, suggesting that the pits are secondaries from this impact crater. The northern and eastern margins of the LLD are located several hundreds of meters away from the chasma edge (Fig. 13), likely due to preferential erosion of the LLD due to its apparently more friable nature. Bedding is not as prevalent in the outcrops on the eastern portion of the deposit, but this may be an artifact of the relative paucity of exposures in this location.

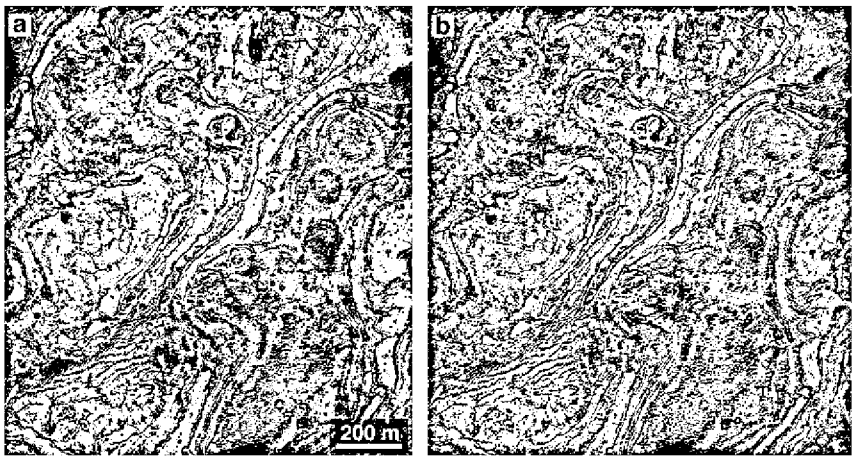

Fig. 11. (a) Example of layering seen in the Melas plateau LLD. Color heterogeneities can be seen between and within beds. Portion of false-color HiRISE image PSP_5729_1700. Illumination is from the left. (b) Stereo anaglyph of the same region shown in (a). Portion of HiRISE images PSP_5729_1700 and PSP_5584_1700. (For interpretation of color mentioned in this figure the reader is referred to the web version of the article.)

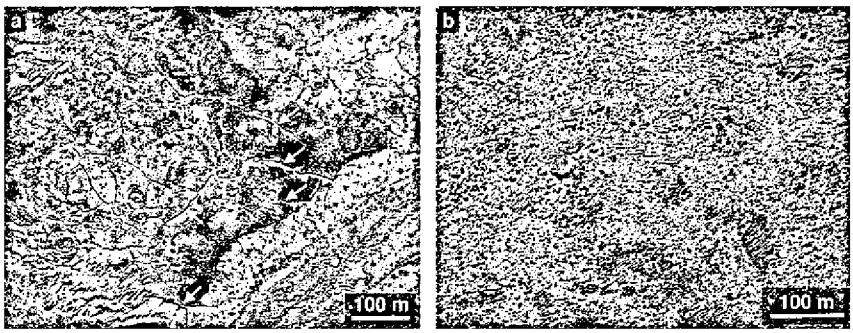

Fig. 12. (a) Linear ridges along the surfaces of layered beds in the Melas LLD. (b) False-color RGB image of pitted upper mantle surface seen on the LLD. The pits could be secondary craters, although the uniform sizes of the pits is unusual for secondaries. The pits are only seen on the dark-toned mantle but not the LLD. Portion of HiRISE image PSP_5729_1700. Illumination is from the left. (For interpretation of color mentioned in this figure the reader is referred to the web version of the article.)

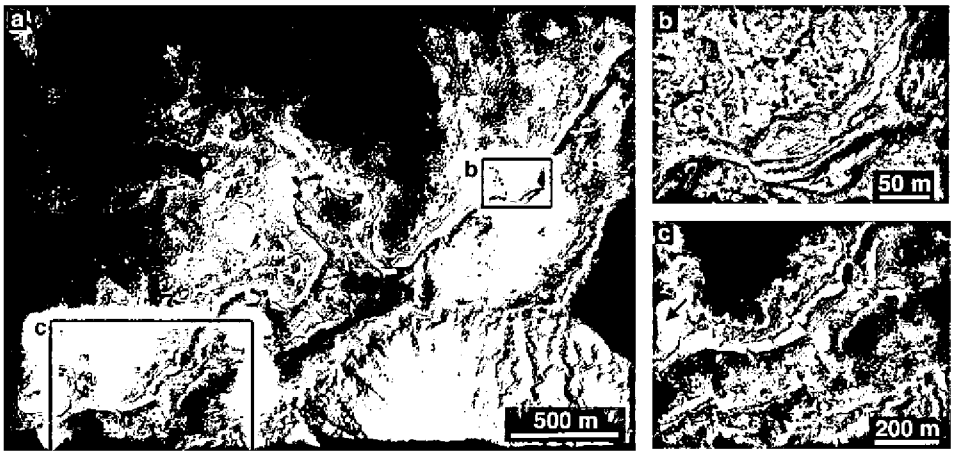

Fig. 13. Eastern edge of Melas LLD. (a) Light-toned layering is best observed along the edge of Melas Chasma. Black boxes indicate locations of blowups shown in (b) and (c). (b) Numerous beds seen along a steep exposure in the LLD. (c) False-color image of the LLD. Black arrow identifies a possible valley. Portion of HiRISE PSP_5030_1685. Illumination is from the left.

4.2. Melas plateau valleys

We have found valley systems in several HiRISE images of the plateau south of Melas, with the best exposed valleys observed in the northeast portion of the LLD. These valleys have typical exposures less than a few hundred meters in length. They have a wispy character and are not well integrated. This may be in part due to limited exposures, but they are not as widespread as at the other locales. Quantin et al. (2005) mapped valley systems within a basin along Melas Chasma, which is just to the north of the LLD on the Melas plateau (Fig. 10). Given their stratigraphic positions and proximity, it is plausible that the valleys seen along the plateau formed at the same time as those within Melas Chasma. Mapping of the valley networks in the Melas Chasma basin by Quantin et al. (2005) suggests these valleys were incised by runoff during a lengthy period of precipitation that may have extended well into the Hesperian. If the valleys we have identified along the Melas plateau formed in association with those found in the Melas basin, then they too could have resulted from sustained precipitation during the Hesperian.

Valleys in the western region of the LLD (Fig. 14a and b) are fine scale (few meters width), space-filling networks consistent with the interpretation that these are first-order tributaries that are rarely observed on Mars (Carr and Malin, 2000). Generally, the drainage direction is from west/northwest to east/southeast in the western HiRISE images. Images acquired further to the east have valleys with third order trunks that indicate a general water flow from the west to east (Fig. 14c). The wider portions of the valleys appear filled with light-toned material, perhaps evaporites or sediments from the waning stages of aqueous transport, whereas the smaller branches appear darker relative to the surrounding LLD in which the valleys incise. A few valleys are located directly next to crater ejecta and the ejecta may have preserved the valleys until they could be exhumed (Fig. 14d). Farther to the northeast, valleys are concentrated along a cliff that runs parallel to the edge of Melas Chasma (Fig. 14e and f). Valleys indicate former flow from south to north along the downslope direction of the cliff, indicating the cliff formed prior to these valleys. MOLA profiles across this portion of the LLD adjacent to the Melas Chasma edge show that it is ~80 m thick.

In a HiRISE image taken adjacent to the Melas Chasma edge, the light-toned layering can be seen within the unit incised by the valleys and the deposit appears to parallel the outline of the chasma edge (Fig. 15). The observation that the valleys incise the LLD implies that they are younger than these deposits and formed after the LLD had been eroded back from the canyon rim. Alternatively, the LLD may not have extended closer to the canyon wall than currently visible and the chasma edge may have acted as a topographic barrier that constrained deposition of the LLD, although there is no evidence of any elevated topography around the chasma edge.

4.3. CRISM results for the Melas plateau

Several CRISM images were acquired concurrently with the HiRISE images over the LLDs south of Melas. Two CRISM HRL images (HRL44AC and HRL7F68) exhibit spectral signatures indic-

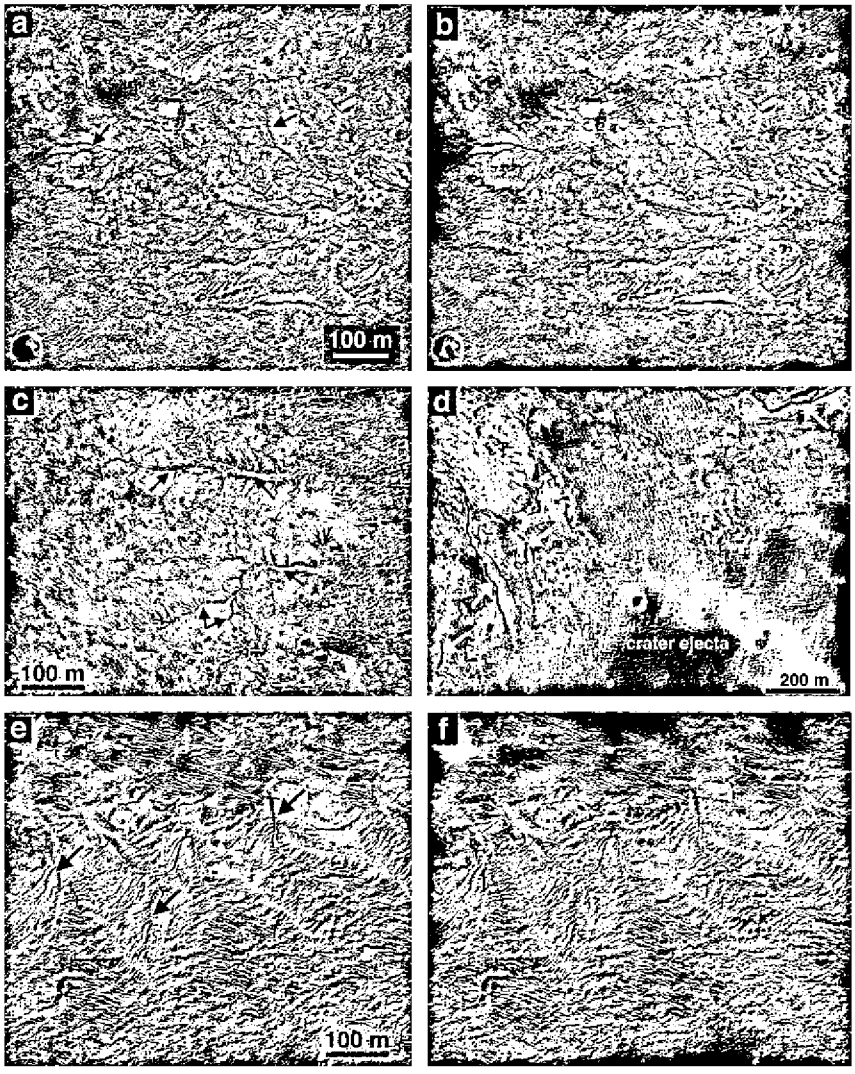

Fig. 14. Examples of valleys seen along the Melas plateau LLD. (a) Valleys (arrows) found in the western portion of the LLD. Flow drainage is to the east. Portion of HiRISE image PSP_5729_1700. Illumination is from the left. (b) Stereo anaglyph of same area shown in (a). Portion of HiRISE stereo pairs PSP_5729_1700 and PSP_5584_1700. (c) Valley branches (arrows) seen in the LLD. The two larger branches are filled with light-toned material while the smaller branches are darker-toned. Direction of water flow is from left to right (west to east). Portion of HiRISE image PSP_6942_1690. Illumination is from the left. (d) Valleys (arrows) incising LLD with a flow direction to the west/northwest. Portion of false-color HiRISE image PSP_9170_1695. Illumination is from the upper left. (e) Valleys (arrows) indicating a downward flow along a cliff at the northern portion of the LLD, adjacent to the Melas Chasma edge. (f) Stereo anaglyph of same area shown in (e). Portion of HiRISE images PSP_9170_1695 and PSP_9803_1695.

ative of opaline silica and jarosite (Fig. 16) (Milliken et al., 2008). Similar to the deposits near Ius, many of the LLD beds appear blue in the CRISM false-color RGB images and lack diagnostic spectral features, whereas the opal-bearing units appear green. In contrast to the LLDs near Ius, the opal-bearing units in this region are darker in HiRISE images (Fig. 16b and d) and are similar in brightness to mantle material on the surrounding volcanic plains. Spectra of the opal-bearing strata in this location exhibit the absorptions discussed previously, most notably a band at ~1.38 μm and a broad band centered at ~2.21 μm (Fig. 16e).

In addition to the opal deposits, other dark-toned deposits exhibit spectra consistent with the presence of non-stoichiometric, Fe-deficient, H_3O-bearing jarosite (Fig. 16b, c, and f) (Milliken et al., 2008). This material is characterized by spectral absorptions near ~1.85 μm and ~2.26 μm. This type of jarosite is associated with low-temperature acidic fluids and does not require high temperatures (e.g., hydrothermal processes) to form, consistent with the interpretation that these LLDs may have formed or been affected by fluvial or other low-temperature aqueous activity. The dark nature of the opal and jarosite units and the absence of clear contacts between these deposits and the LLD make it difficult to ascertain whether these minerals are in the bedrock or occur as thin surface coatings in this location. Both minerals are found at the same stratigraphic level of the LLD (i.e. above the lava plains) but they could have been deposited before or after emplacement of the LLD. This is the only deposit of the five Valles Marineris plateau LLDs examined that exhibits clear evidence for jarosite.

5. Candor plateau

5.1. Candor plateau LLD

The LLD is situated on the plateau between southwestern Candor Chasma and northwestern Melas Chasma (Fig. 17). The best exposures of light-toned layering and valleys occur in the western parts of the LLD (Fig. 18a). We estimate the thickness of the deposit to be ~20–30 m based upon MOLA profiles. Much of the deposit is

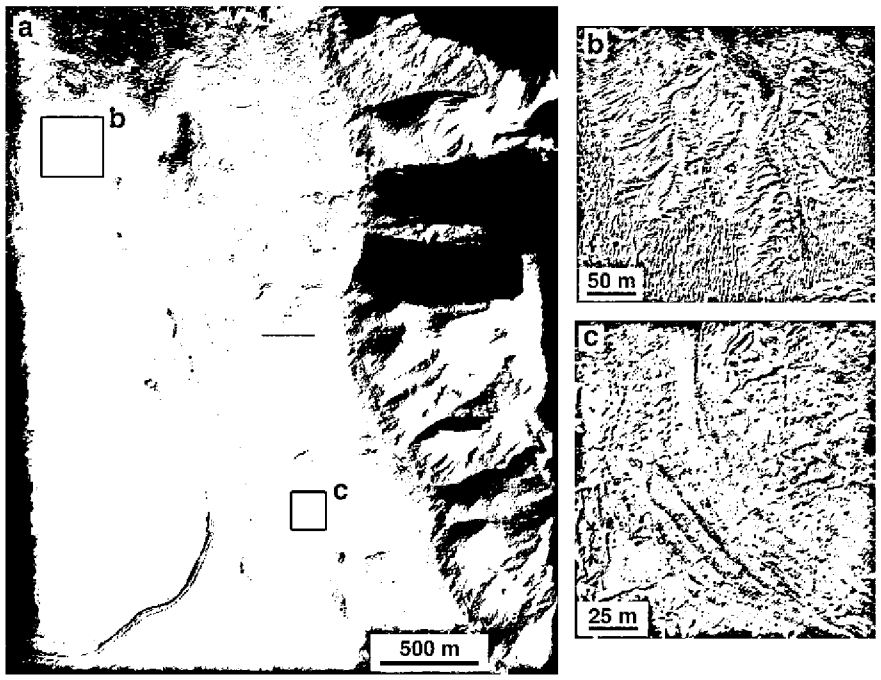

Fig. 15. (a) Valleys and layering along the plateau directly adjacent to Melas Chasma. The Melas Chasma wallrock is in the right of the image. The edge of the LLD is several hundreds of meters from the edge of the chasma, either because it has been eroded back or it was never deposited closer to the chasma edge. Blowups shown in (b) and (c) are identified by black boxes. (b) Blowup of valleys along a cliff in the LLD. Drainage direction is to the north. (c) Beds seen in a steep exposure along the LLD. Portion of HiRISE image PSP_9948_1700. Illumination is from the upper left.

buried underneath a dark-toned mantle with eolian bedforms, although the patchiness of LLD exposures may also result from lateral discontinuities in deposition. Although HiRISE images currently only cover the central and northern portions of the LLD, CTX images to the south that are adjacent to Melas Chasma show light-toned layered material that we have mapped as possible LLD (Fig. 17).

Northwest-trending grabens cut across the plateau for hundreds of kms and can be up to 700 m deep. Several of these grabens can be traced to the head of tributary canyons on the northern edge of Melas Chasma. The interiors of the grabens have limited exposures of LLD, although the floors are covered with ripples and eolian debris that could be obscuring the LLDs in these topographic lows. Rocks exposed along the graben walls are morphologically similar to layers that are observed along the upper chasmata wallrock and interpreted as Hesperian volcanic plains materials.

Polygonal fracturing is visible on some of the light-toned beds. There are numerous bulls-eye patterns in the LLD (Fig. 18b), either resulting from scouring of hollows by the wind or from former impact craters that were filled in by sediment. The morphology of the layered beds is similar to those found along the Ius and Melas plateaus, although there appear to be fewer color variations between individual beds. Beds in the LLD near the southern edge of west Candor Chasma appear broken up and pinched, suggesting disruption either during or after emplacement.

Polygonal cracks and ridges are evident in many of the underlying lava plains units (Fig. 19a). The size of these polygons ranges from 10 to 30 m, which is larger than the meter-size polygons seen on the overlying light-toned beds. Additionally, polygonal cracks in the lava plains have a pronounced rectilinear pattern that differs from the more equant polygonal pattern observed on the LLD. The volcanic plains near the edge of west Candor Chasma have a light-toned surface, but lack clear evidence of layering. This type of light-toned surface may result from chemical alteration and is seen elsewhere along the Valles Marineris plateau (see Section 7.3).

We have identified two light-toned beds on the floor of a ~6 km diameter impact crater that differ in both brightness and color (Fig. 19b). These outcrops lack polygonal fracturing and do not exhibit fine-scale bedding as is typical for outcrops in the LLD. These two units may not be the same LLD seen outside the crater along the volcanic plains.

Stereo pairs of HiRISE images reveal that the LLD can be concentrated in local topographic lows along the lava plains and in grabens (Fig. 20). This observation would argue against an explosive or airfall origin for these deposits and favor depositional mechanisms that would collect material in low-lying regions (e.g., aqueous or eolian processes). Alternatively, erosion has removed the LLD from higher regions but the deposit is preserved in these low-lying regions.

5.2. Candor plateau valleys

Few examples of valleys are found in the LLD at this site, with all known examples in the northwestern portion of the deposit. They incise predominantly the LLD with only a few present along the dark-toned lava plains. The valleys have a dendritic pattern and are space-filling. Exposures of the valley systems are discontinuous and occur in windows through the overlying eolian mantle that are typically a few hundred meters across; therefore, the extent of network development is difficult to quantify but reaches at least third order. Valleys and older impact craters are filled with dark-toned eolian debris. The valleys suggest a former drainage direction to the south (Fig. 18a), consistent with MOLA profiles that indicate a regional surface slope in this direction. The limited expression of fluvial landforms within the LLD appears related both to restricted preservation and exposure, as well as limited development. That is, fluvial dissection does not appear to be common within the LLD and is confined to specific layers. At least one example has LLD material locally obscuring a portion of the valley network indicating that formation of this system occurred during the period of LLD formation.

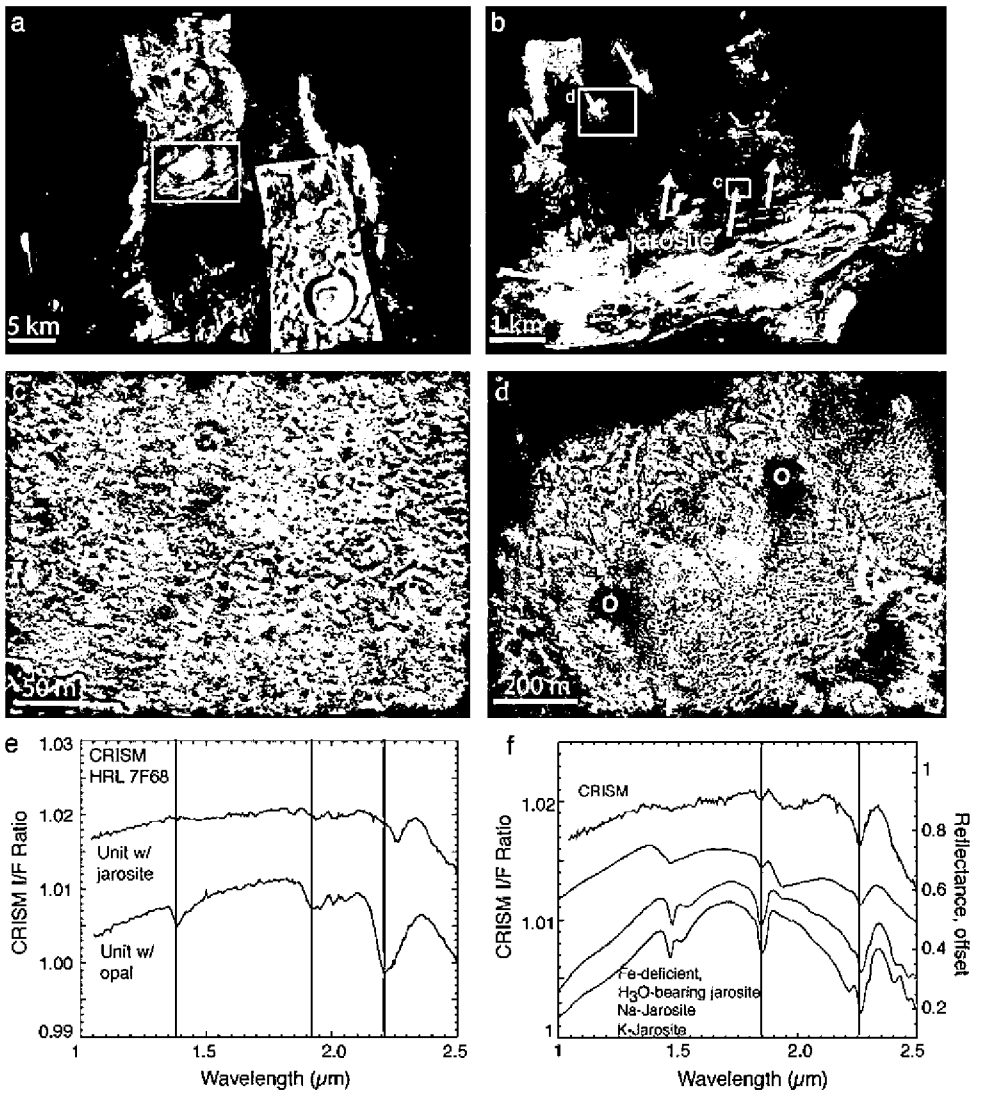

Fig. 16. (a) An example of two false-color CRISM images overlaid on a CTX mosaic. The bluish-greenish colors in the CRISM image correspond to the outcrops of LLD. The white box outlines the region in (b). (b) Close-up of a CTX image showing the approximate locations of the opal and jarosite deposits whose spectra are presented in (e). Note that the hydrated minerals occur in relatively dark-toned materials, unlike the observations near Ius. (c) Portion of HiRISE image PSP_005518_1690 showing the unit containing jarosite. Illumination is from the left. (d) The opal deposits (o) in a portion of false-color HiRISE image PSP_005518_1690. Illumination is from the left. (e) Ratio spectra from the upper left CRISM image in (a) based on pixel averages corresponding to the units marked by arrows in (b). The green spectrum is shown in detail in (f), a comparison to laboratory jarosite spectra. (For interpretation of color mentioned in this figure the reader is referred to the web version of the article.)

5.3. CRISM results for the Candor plateau LLD

There is a strong correlation between light-toned beds in HiRISE images and bluish deposits in CRISM false-color images (Fig. 21). Similar to other LLD localities, green colors in the CRISM images correspond to opal-bearing units (Fig. 21a and b). The opal units have a brightness that is intermediate between the brighter LLD beds and the darker lava plains material. The unit generally has larger scale (10–30 m) polygonal fracturing than seen in the LLDs (Fig. 21c), and it is commonly found closer to the edges of grabens and canyons than the brighter LLD beds. Averaging CRISM pixels from the bluish units in Fig. 21a indicates there is a hydrated phase in these beds (Fig. 21b). The spectral signature of this phase is extremely weak, making it difficult to determine band positions and shapes at a statistically significant level. Therefore, although this hydrated phase may be opaline silica, a unique identification is impractical and we can only state that these beds contain a hydrated phase. This detection suggests the similar light-toned beds (bluish in the CRISM false-color RGBs) observed at other locales may also contain a hydrated phase and that the outcrops are simply too small to uniquely characterize these phases at the resolution of CRISM. However, additional data and further investigation of those outcrops is needed to test this hypothesis. As shown in Fig. 21d, the outcrops of LLDs are interspersed between eolian materials, which complicates the spectral extraction of a pure LLD component. We have not yet detected evidence for sulfates or other hydrated salts in this location.

6. Juventae plateau

6.1. Juventae plateau LLD

The Juventae plateau LLD is divided into three components, with the best exposures of the deposit concentrated around the northern and southern portions of an isolated 17 km wide, 1.7 km deep pit that is about 20 km west of Juventae Chasma (Fig. 22). Smaller exposures of light-toned layering occur beneath preserved crater ejecta and inside inverted channels. The plateau

Fig. 17. CTX mosaic of the plateau between West Candor Chasma and Melas Chasma. We have mapped areas where light-toned layering outcrops are visible in CTX and/or HiRISE images by purple color while likely locations of LLD seen in CTX images are mapped in brown. Black boxes identify HiRISE images and yellow boxes show locations of later figures. Drainage directions seen in valley networks are shown by arrows. Illumination is from the left. (For interpretation of color mentioned in this figure the reader is referred to the web version of the article.)

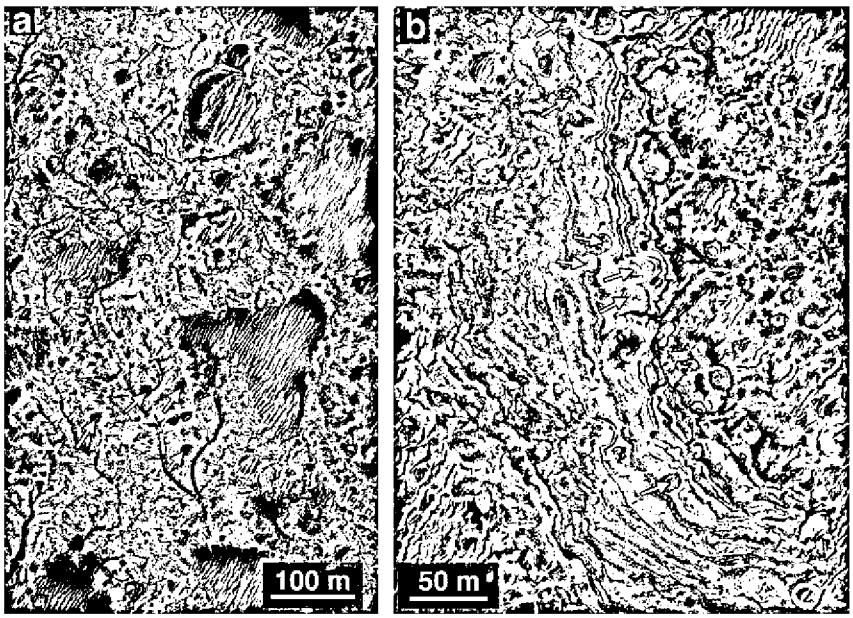

Fig. 18. (a) False-color HiRISE image of valleys incised into the Candor plateau LLD. Dark-filled impact craters are shown by yellow arrows. Portion of HiRISE image PSP_6731_1730. Illumination is from the upper left. (b) Example of layering seen within the LLD. Bulls-eye pattern in the LLD (yellow arrows) could result from scouring of hollows or former craters that filled in with light-toned layered material. Portion of HiRISE image PSP_7588_1730. Illumination is from the upper left. (For interpretation of color mentioned in this figure the reader is referred to the web version of the article.)

LLD does not extend to the trough edge but instead appears to be eroded back tens of meters by the wind, likely reflecting its relatively friable nature. MOLA profiles across the LLD indicate it is ~50 m thick, although the thickness varies depending upon the extent of erosion. A Digital Terrain Model (DTM) generated using two HiRISE images (Kirk and 18 colleagues, 2008) of the LLD (Fig. 23) allows us to determine a 60 m thickness for the strata at this location, and bedding appears parallel across the width of the DTM, except where it is disrupted by impact craters. MOLA profiles over the entire region show the surface topography of the LLD is variable, however, with the lava plains and LLD in the north having lower elevations than those to the south (Fig. 24). Either the LLD was deposited on formerly horizontal topography that was subsequently modified by uplift or downdrop portions of the LLD in association with the formation of the pit, deposition occurred at multiple topographic levels, or the LLD dips to the north. We note that the LLD appears to have been diverted around an east–west trending wrinkle ridge located just southeast of the pit (Fig. 22, blue arrows), an observation that would support fluvial and eolian origins.

Strata in the Juventae LLD share characteristics with the other plateau LLDs, including brightness, color, and surface variations (Fig. 25) (Lucchitta, 2005). In addition, there are excellent cliff-bench exposures along most of the LLD, with typical downhill surface slopes of 5–15° derived from the DTM. Polygonal fractures are commonly found on the surfaces and vary in size and shape for

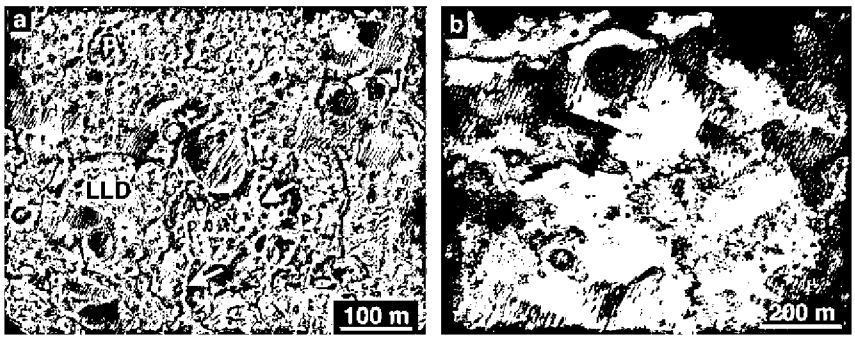

Fig. 19. (a) Contact between underlying lava plains (P) and the LLD. The upper surface of the lava plains appears light-toned, perhaps due to weathering. Yellow arrows show polygonal ridges in the plains. Portion of HiRISE RGB image PSP_6731_1730. Illumination is from the upper left. (b) Light-toned and medium-toned units found on the floor of an impact crater. The two units appear morphologically distinct from the LLD. Portion of HiRISE RGB image PSP_4318_1730. Illumination is from the left. (For interpretation of color mentioned in this figure the reader is referred to the web version of the article.)

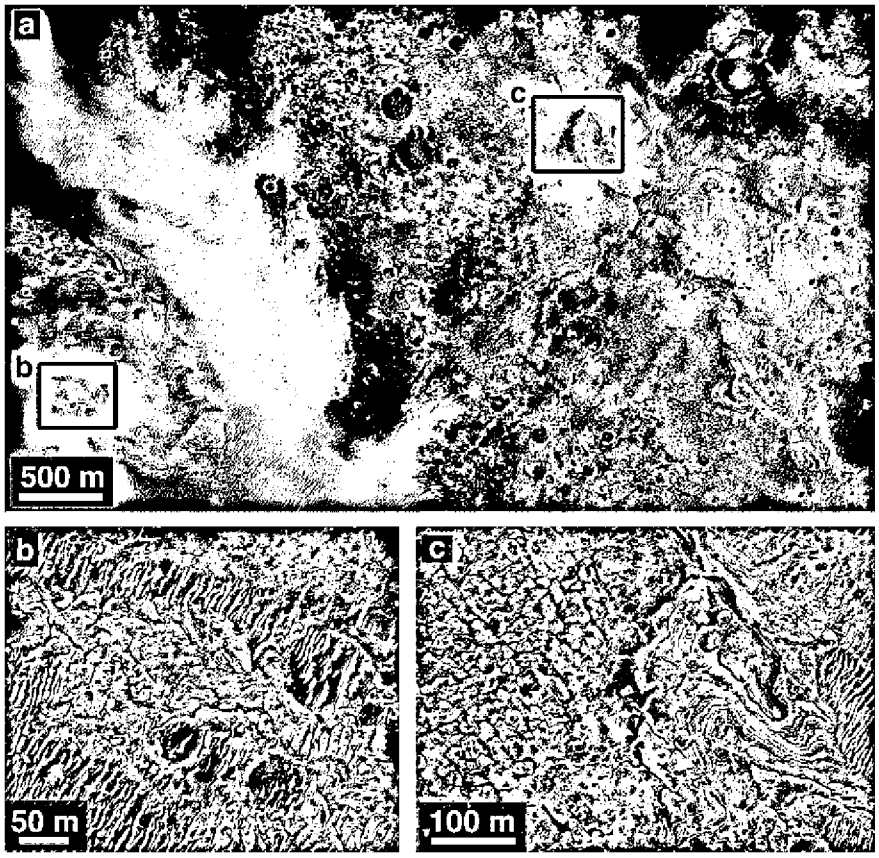

Fig. 20. (a) Stereo anaglyph of the plateau between Melas and Candor chasmata. The LLD is found in local topographic depressions. Black boxes identify locations of blowups shown in (b) and (c). Portion of HiRISE images PSP_4318_1730 and PSP_4740_1730. Illumination is from the left. (b) LLD along the floor of a graben. (c) LLD and polygonally fractured volcanic plains.

individual beds (Le Deit et al., 2008b). In several locations, the fractures are not polygonal in shape, possibly a result of cracking attributed to breakage and erosion of that layer. It appears that beds with similar characteristics (such as the sizes of polygonal fractures or those lacking polygonal fractures) repeat throughout an exposed sequence, suggesting a cyclic process for deposition. We find no apparent change in the thickness of the beds when they can be traced over several kilometers. Ridges in the LLD can trend downslope, perpendicular to the horizontal strata bedding. These ridges define edges of arcs where strata stick out and therefore represent erosional ridges rather than depositional features (Fig. 25).

In addition to the LLD observed on the plateau here, we have also identified a LLD on the central floor of a pit near Juventae Chasma (blue region in Fig. 22). While ILDs inside the chasmata stand as mounds above the adjacent chasma floor, this light-toned layered deposit lies at the lowest elevation on the pit floor. The exposure of layering appears to be the result of collapse associated with formation of the pit and subsequent erosion by wind scouring along the pit's floor. There is no evidence for fluvial dissection of the wall surrounding the pit. The layering in the pit's wallrock appears morphologically similar to the lava plains seen along the Juventae Chasma wallrock. In contrast, the layers in this pit LLD

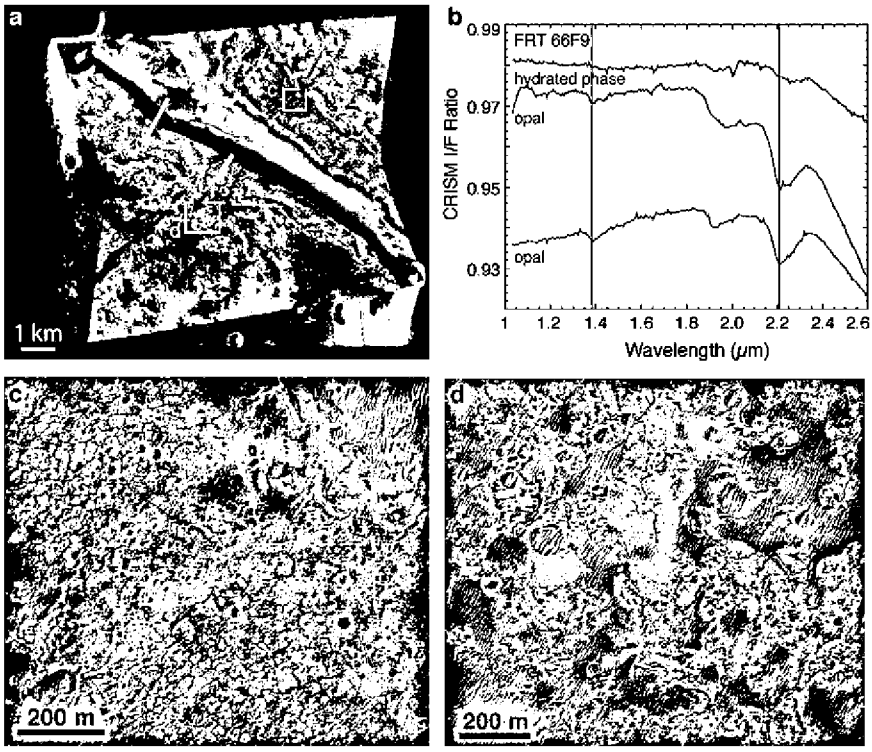

Fig. 21. (a) Close-up of CRISM FRT 66F9 with blue and green tones corresponding to LLD outcrops. The green color (green and red arrows) indicate opal-bearing material, whereas the blue arrow indicates bluish material that exhibits very weak hydration features. The dashed yellow line marks the boundary between these two units, showing that the opaline material is closer to the graben. (b) CRISM ratio spectra corresponding to the arrows in (a). The greenish materials in (a) clearly have opal, whereas it is difficult to identify the specific hydrated phase in the bluish materials. (c) Portion of HiRISE image PSP_004740_1730 showing the opaline material that corresponds to the spectra in (b). The surface is rugged with polygonal fracturing at a larger scale than seen in the LLDs. (d) Blowup of the LLD where the spectra shown in blue (b) were taken. Portion of HiRISE image PSP_004740_1730. Illumination is from the left. (For interpretation of color mentioned in this figure the reader is referred to the web version of the article.)

resemble the plateau LLD rather than the ILDs seen within Juventae Chasma (Fig. 26). Although the contacts between the LLD and wallrock are commonly obscured by debris, a HiRISE stereo pair reveals the LLD is topographically lower than the wallrock and spurs, suggesting it may also be stratigraphically lower than the wallrock (Fig. 26b). If true, this LLD would be older and represent an episode of deposition that is distinct from the plateau LLD.

6.2. Juventae plateau fluvial landforms

Inverted channels (ICs) are clustered in two locations along the plateau adjacent to Juventae Chasma (Fig. 22). Although mapped as 'IC' in Fig. 22, the unit also contains LLD both within and adjacent to the inverted channels. Using MOC images, Williams et al. (2005) identified four discreet third- and fourth-order stream networks that have drainage densities among the highest observed on Mars (0.9–2.3 km^{-1}). There are no recognizable ICs within the larger exposures of LLD, but we can identify ICs along the edges of LLD where there has been sufficient differential erosion to expose them (Fig. 27). HiRISE images of the ICs show that they contain light-toned beds (Fig. 27) that appear to be the same as those within the LLD, sharing the same color and brightness variations between layers, polygonal fractures, and erosional properties. Most of the ICs indicate a former water flow consistent with the 0.2° regional slope downwards to the northeast (Mangold et al., 2008). However, many ICs do not follow this regional trend but instead suggest a localized slope that caused a preferred orientation (e.g., Fig. 27a). Moving eastward, the ICs have a more northerly direction that does not follow the current regional surface slope, perhaps reflecting tectonic tilting after their emplacement. Stereo HiRISE images reveal that any individual IC varies in height along its length, likely due to differential erosion. MOLA profiles across several ICs indicate a typical height of ~20 m.

The ICs could have formed when less resistant material surrounding the valleys differentially eroded to expose the layered sediment that filled the valleys (Williams et al., 2005; Pain et al., 2007; Mangold et al., 2008). Alternatively, inverted streams could represent sediment deposited beneath a former glacier by basal melting in which subsequent melting or ablation of the glacier allowed the streams to obtain the positive topography characteristic of eskers. Mangold et al. (2008) note that there are no glacial landforms seen on the Juventae plateau and the ICs increase in size as they connect to other ICs, characteristics that would not support a glacial origin. Instead, the orientation and organization of the ICs favor fluvial deposition within channels followed by eolian removal of surrounding less resistant material. The sediment within the former streams may also have been preferentially cemented by late fluid circulation, causing these deposits to be more resistant to erosion.

The stratigraphic relation of the fluvial landforms at this site is particularly noteworthy. Fig. 27b illustrates that the ICs are present at multiple stratigraphic horizons with the broadly sinuous branching ridgeform trending roughly SW–NE stratigraphically beneath the dendritic branching ridge network that trends W–E. In addition to the ICs, we have identified negative relief valleys that incise the lava plains and have no associated LLD (Fig. 28). The negative relief valleys lie beneath and have a different flow direction than a younger IC. The negative valleys could either represent an older period of aqueous activity or they could be former ICs where all the sediment has been completely eroded. In the northwest por-

Fig. 22. CTX mosaic of the Juventae plateau LLD. The LLD is mapped in purple, possible LLD preserved beneath crater ejecta is mapped in brown, units dominated by inverted channels (IC) are mapped in green, and a light-toned layered deposit found on the floor of a pit is mapped in blue. Interior layered deposits (ILD) can be seen as mounds on the floor of Juventae Chasma. The locations of HiRISE images are shown by white boxes and the MOLA profile shown in Fig. 24 is noted by the red line. Yellow boxes indicate locations of later figures. Black arrows show inferred drainage direction for the inverted channels and valleys. Blue arrows identify a wrinkle ridge that the LLD appears to have been diverted around during emplacement. Illumination is from the left. (For interpretation of color mentioned in this figure the reader is referred to the web version of the article.)

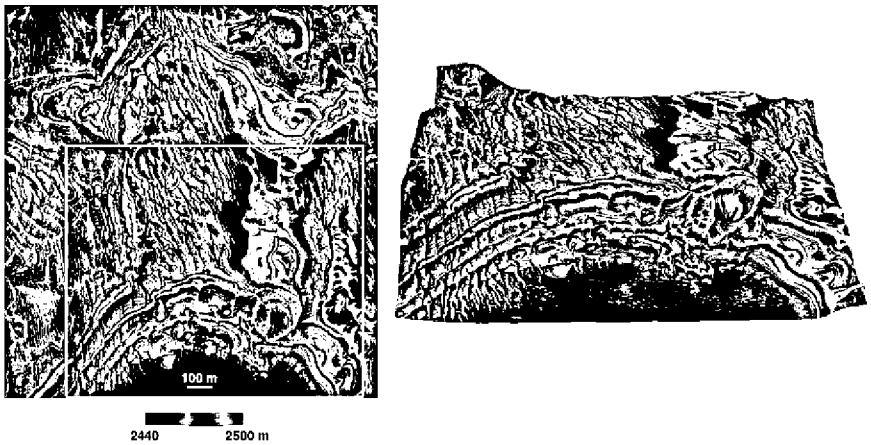

Fig. 23. Portion of HiRISE image PSP_3579_1755 overlain with DTM-derived topography shown in color. Contours spaced at 5-m intervals can be seen in magenta. The yellow box outlines the location of the DTM shown to the right, which has 7× vertical exaggeration. Illumination is from the left. (For interpretation of color mentioned in this figure the reader is referred to the web version of the article.)

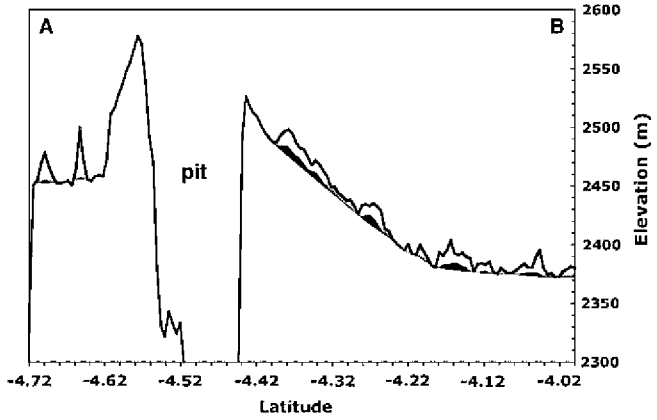

Fig. 24. MOLA PEDR ap15277 across the Juventae plateau LLD. The LLD (gray) decreases in elevation moving to the north (see Fig. 22 for location of profile). Vertical exaggeration is 138×. The average slope of the terrain north of the pit is only 0.5° and could be the result of uplift during formation of the pit.

tion of the LLD we have found channels that lie within larger ones (Fig. 29). From these observations, we deduce that multiple periods of fluvial activity occurred in this region during the Hesperian.

After examining both CTX and HiRISE images, we have found valleys and ICs along the Juventae chasma wall (Fig. 30) only a few kilometers south of the LLD on the plateau. Light-toned layering is also associated with these ICs in the HiRISE images (Fig. 30c). Because the exposures of light-toned layering are small, we cannot determine if they represent the same materials seen in the LLD along the plateau. The only other chasma location where we have seen similar fluvial landforms and light-toned material along the walls is in southwestern Melas Chasma, which also has valleys and LLD on the plateau above (Fig. 10). In both locations, we believe the precipitation and surface runoff that formed the valleys on the plateau also produced the valleys seen along the adjacent wallrock, suggesting a larger area of precipitation than the more localized episodes previously suggested by others (e.g., Quantin et al., 2005; Mangold et al., 2008). If the spatially proximal valleys along the chasmata walls and plateau are coeval, then their formation occurred after creation of the chasmata, perhaps in the mid-Hesperian, although we note that there were likely several episodes of hydrologic activity associated with the fluvial landforms on the lava plains and so there could also be older periods of water flow.

6.3. CRISM results for the Juventae plateau LLD

CRISM spectra of the LLD on the plateau adjacent to Juventae Chasma exhibit absorptions consistent with the presence of opaline silica and partially dehydrated Fe-sulfates (Milliken et al., 2008; Bishop et al., 2009). Similar to other locations, these finely-stratified deposits appear bluish-green in CRISM false-color RGB images (Fig. 31) and are distinct from the nearby sulfate-rich ILDs within Juventae Chasma. The HiRISE color variations of adjacent beds of the Fe-sulfate unit, which corresponds to the finely layered beds within the LLD, and the slight variations in CRISM spectral signatures observed for this unit suggest that multiple related phases might be present. Opal-bearing materials are commonly darker and appear to be stratigraphically lower than the sulfate-bearing beds (Fig. 31c), a sequence consistent with evaporation of fluids produced by acidic weathering of a basaltic precursor (Milliken et al., 2008). In particular, Milliken et al. (2008) showed that the light-toned, finely-stratified deposits have spectra similar to a partially dehydrated ferricopiapite (Fig. 31d and f), although other Fe-sulfates may exhibit similar spectral properties upon dehydration. This material exhibits a narrow absorption at

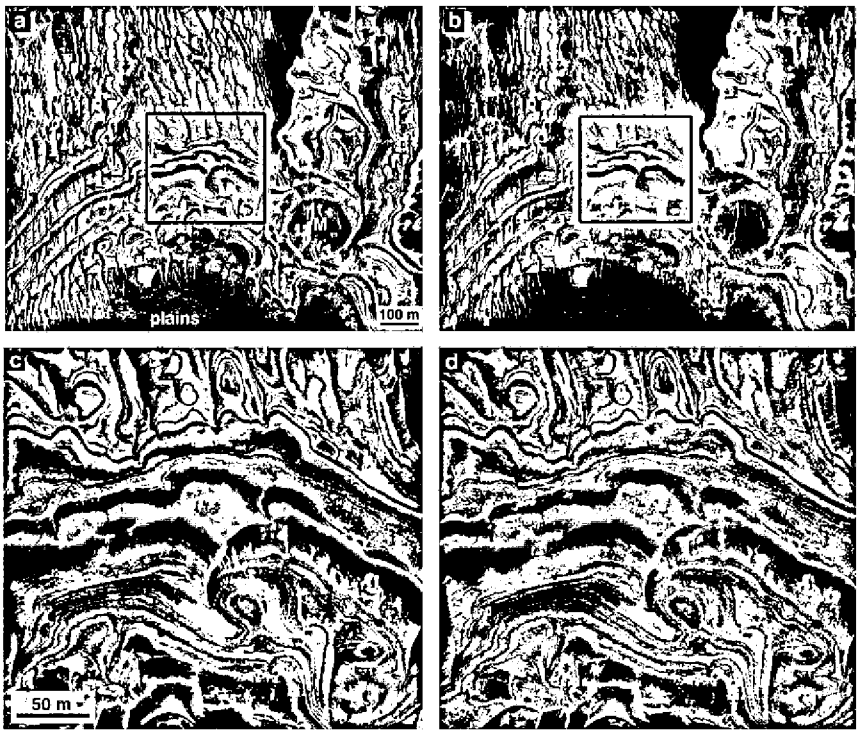

Fig. 25. (a) Examples of layering in the Juventae plateau LLD. Vertical ridges in the strata are indicated by red arrows. A brown mantle (M) covers portions of the LLD. Black box identifies location of blowup shown in (c). Portion of HiRISE RGB image PSP_3579_1755. Illumination is from the lower left. (b) Stereo anaglyph of the same area shown in (a). Black box identifies location of blowup in (d). Portion of HiRISE images PSP_3579_1755 and PSP_3434_1755. (c) Color variations and (d) cliff-bench morphology in the LLD. (For interpretation of color mentioned in this figure the reader is referred to the web version of the article.)

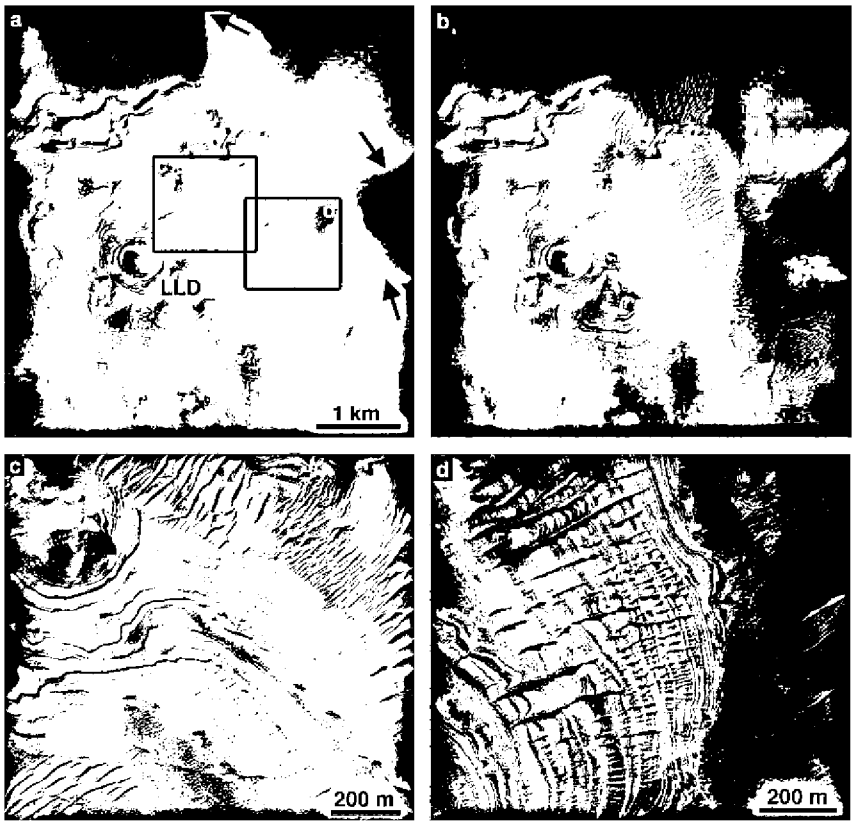

Fig. 26. LLD along the floor of a pit next to Juventae Chasma. (a) Geologic contact between wallrock spurs (black arrows) composed of volcanic plains materials and the LLD. Black boxes identify blowups shown in (c) and (d). Portion of HiRISE image PSP_9130_1755. Illumination is from the upper left. (b) Stereo anaglyph of the same area shown in (a) provides compelling evidence for the LLD lying beneath the wallrock and therefore representing an older deposit relative to the LLD along the plateau. Portion of HiRISE images PSP_9130_1755 and PSP_9842_1755. (c) The beds within the LLD do not display as many color or brightness variations as those along the plateau but eolian debris may cover these low-lying beds. (d) Portion of HiRISE RGB image PSP_4990_1755 shows the light-toned nature of the beds, polygonal fracturing, and brightness and color variations in the uppermost strata that are characteristic of the LLD along the plateau. Illumination is from the left. (For interpretation of color mentioned in this figure the reader is referred to the web version of the article.)

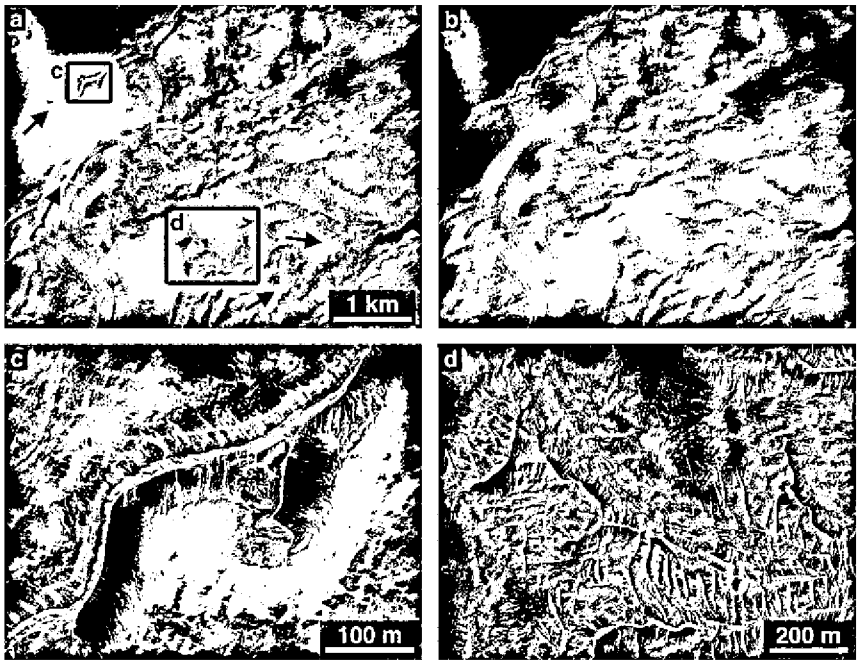

Fig. 27. (a) Inverted channels along the plateau adjacent to Juventae Chasma. Arrows indicate drainage direction to the east and northeast. Black boxes show locations of blowups. Portion of HiRISE image PSP_6981_1760. Illumination is from the left. (b) Stereo anaglyph of same area shown in (a). The upper surfaces of the ICs vary in height both along the IC and relative to neighboring ICs. (c) Blowup of an IC. Light-toned layering is visible within the IC. (d) RGB image of light-toned layering within ICs. (For interpretation of color mentioned in this figure the reader is referred to the web version of the article.)

Fig. 28. Portion of HiRISE RGB image PSP_5346_1755 showing older negative relief channels (white arrows) beneath younger inverted channel (yellow arrow). Arrows indicate likely flow direction. Illumination is from the left. (For interpretation of color mentioned in this figure the reader is referred to the web version of the article.)

~2.23 μm that is relatively uncommon for geologic materials, a shoulder near 2.4 μm and a water band near ~1.93 μm. The opaline silica-bearing materials appear cracked and fragmented. They are found at the contact between the older volcanic plains surface and the younger LLD, and could either represent the lowermost stratigraphy in the LLD or the uppermost surface of the lava plains.

As discussed above, the LLD exposed in the pit west of Juventae are partially covered by eolian debris and dust, making it difficult to retrieve their composition at the spatial resolution of CRISM. However, averaging the pixels for all of the layers (red arrow in Fig. 31a) and dividing by the spectrum from a dusty region produces a ratio spectrum consistent with jarosite (Fig. 31e). Although the absorption features are weak, a relatively narrow band centered at 2.26 μm and a broad asymmetric band near 1.93 μm are similar to the jarosite spectra detected south of Melas (shown in Fig. 16). The lack of a downturn at wavelengths shorter than ~1.5 μm (Fig. 31e) may be an artifact of the ratio method or a result of very thin coatings that only affect the shortest wavelengths. Additional observations of layers within this pit are needed to verify this detection, but it is clear that the spectral signatures of the LLD within the pit are different from the LLD on the surrounding volcanic plains.

7. Ganges plateau

7.1. Ganges plateau LLD

The Ganges plateau LLD is located along the western edge of Ganges Chasma (Fig. 32). It is the smallest of the five VM plateaus LLDs and has the fewest exposures of light-toned strata due to a blanket of darker-toned material that obscures most of the LLD (Le Deit, et al., 2009) (Fig. 33). The dark mantle could be eolian or impact materials or debris derived from weathering of the surfaces of the LLD. The LLD is considerably cooler relative to surrounding terrain in THEMIS nighttime IR images (Le Deit, et al., 2009) indicating the presence of finer-grained material that are not found on the lava plains. The LLD may have once extended to

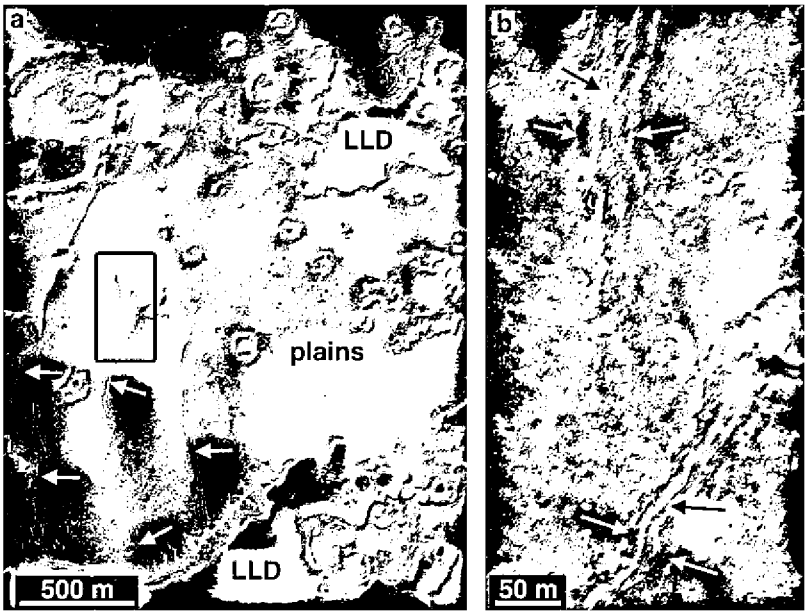

Fig. 29. (a) The northernmost exposure of the mapped LLD has lava plains with channels that contain smaller channels (white arrows), suggesting at least two episodes of surface flow. Black box shows blowup in (b) where inner channels are marked by black arrows and white arrows identify outer channel. The inner channel at the bottom of the image appears filled in and could be inverted. Portion of HiRISE image PSP_7482_1760. Illumination is from the upper left.

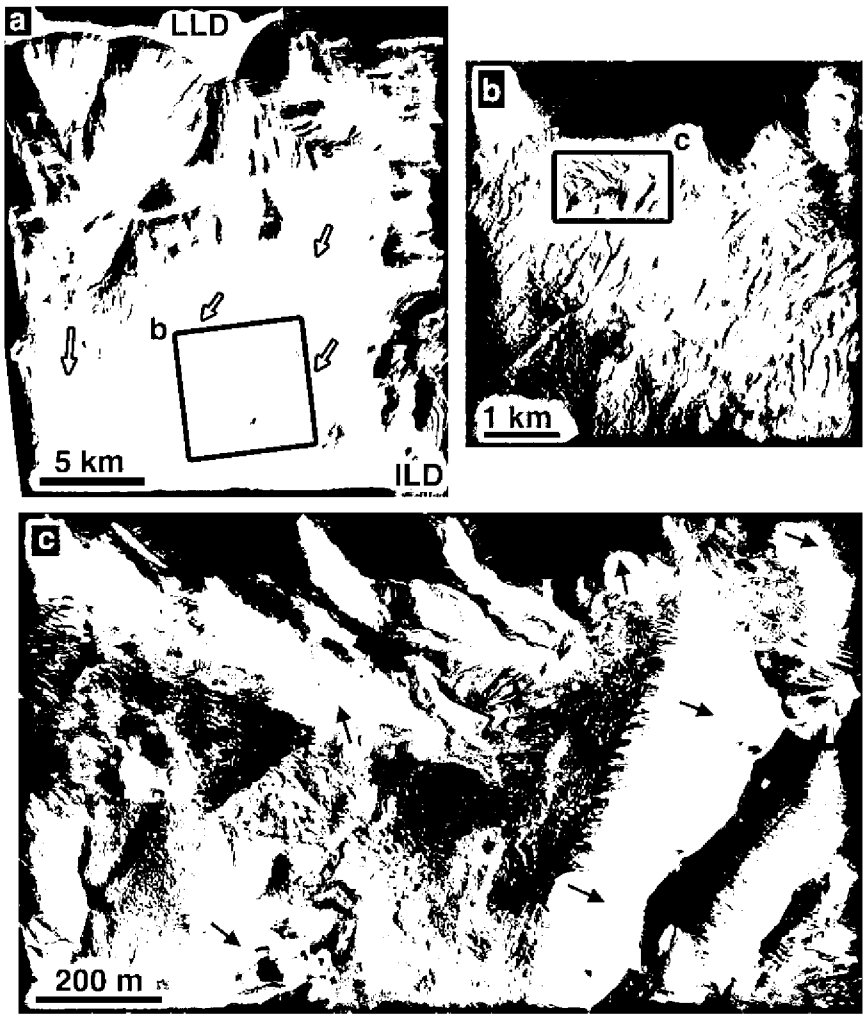

Fig. 30. (a) Inverted channels and valleys along the northern Juventae Chasma wall. Drainage direction is indicated by black arrows. Black box outlines location of blowup shown in (b). Portion of CTX image P03_2234_1761. Illumination is from the left. (b) Valleys and inverted channels near the bottom of the wall. Portion of HiRISE image ESP_011688_1760. Illumination is from the left. (c) Light-toned layering (black arrows) contained within inverted channels. Portion of HiRISE image ESP_011688_1760.

the chasma edge but it is now located tens of meters away, presumably due to eolian erosion. A 5.5-km diameter crater and its ejecta are superimposed on the LLD and have caused destruction and disruption of the LLD surface. MOLA profiles across the LLD can be used to infer a thickness of 20–50 m at present. Where exposures are large enough to examine multiple layers, the morphology of the LLD is comparable to the other plateau LLDs, with a diversity of brightness, color, polygonal fracturing, and erosional properties for individual beds within the strata (Fig. 34).

7.2. Ganges plateau valleys and inverted channels

The Ganges plateau LLD is located at the terminus of one branch of the 190-km long Allegheny Vallis system (Fig. 32). The flows from Alleghany Vallis are believed to have occurred in the mid- to late-Hesperian (Coleman et al., 2007) and were sourced from a 37-km long and 2-km deep pit called Ophir Cavus. MOLA data show the typical depth of Allegheny Vallis to be ~100 m, with some portions shallower than others. The floor of the outflow channel has a regional slope of 0.2° and descends ~0.5 km in elevation from the west to east. The branch that extends to the LLD is shallower than the main channel that continues to the south and has a segment that appears to be captured by a tributary canyon of Ganges Chasma (Fig. 32) (Harrison and Grimm, 2005; Coleman et al., 2007). There is no LLD associated with this deeper southern channel, although continued extension and mass wasting along the chasma walls may have removed or buried any LLD that may have been present at the eastern extent of this main channel. An extensive outflow channel (Elaver Vallis) also exists to the southeast (Coleman et al., 2007) and there is a small valley and associated terraced fan in a crater to the southwest of the LLD, indicating widespread aqueous activity on the plateau adjacent to western Ganges Chasma during the Hesperian.

Isolated ridge segments associated with the LLD are similar in scale and form to inverted channels (Fig. 35), such as those observed near Juventae Chasma. Light-toned layering is observed beneath the ridge surface in these inferred inverted channels, as is evident in inverted channels elsewhere associated with the LLDs (e.g., Fig. 27). The largest IC can be seen extending 4 km outside the LLD and into a branch of Allegheny Vallis (Fig. 36). This IC can also be traced into the LLD ~11 km. Lineations feather out from this IC in the north–south directions at high angles (Fig. 36b). Similar lineations with high branch angles are found in association with postulated subaqueous deposition fans in Melas Chasma (Metz et al., 2009), although the fans at Melas also have lobe-shaped terminations and occur within a closed basin interpreted as the site of a former paleolake (Quantin et al., 2005), neither of which are observed in the Ganges plateau LLD. Consequently, the

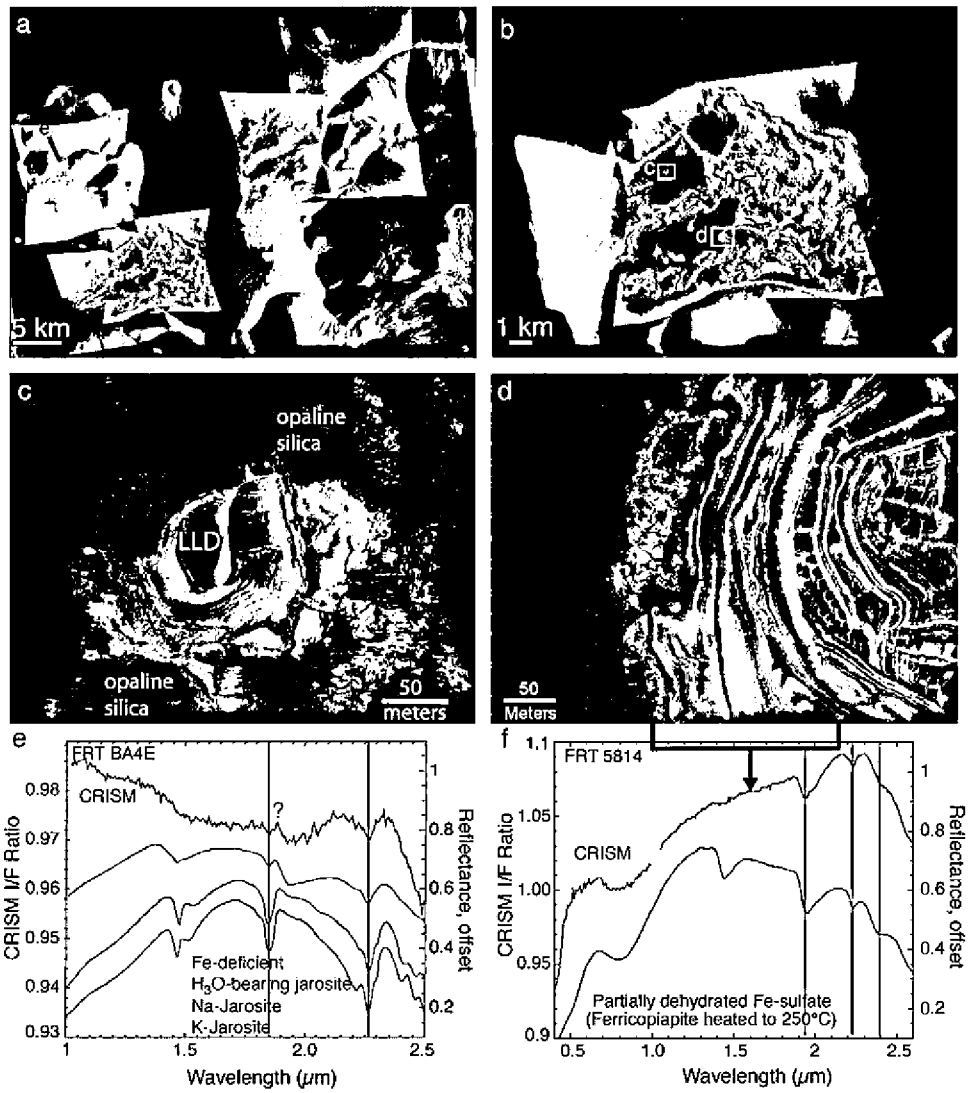

Fig. 31. (a) CTX mosaic with CRISM false-color images superimposed. The LLD outcrops appear bluish in these images. The red arrow marked 'e' indicates the location of the ratio spectrum shown in (e). (b) CRISM FRT 5814 overlaid on CTX image. White boxes identify locations of blowups. (c) Blowup of opaline silica exposures in HiRISE image PSP_003579_1755. Opaline silica is located stratigraphically beneath the LLD and is only exposed where erosion has removed the overlying LLD. Illumination is from the lower left. (d) HiRISE false-color image showing a close-up of the finely-stratified LLD. The bottom beds in this outcrop and other adjacent outcrops exhibit spectra consistent with Fe-sulfates. (e) Ratio spectrum of LLD in the pit west of Juventae (CRISM FRTBA4E). Although not as clear as the jarosite spectrum in Fig. 16, this spectrum shares many of the same attributes, most notably a narrow band centered at 2.26 μm and a broad asymmetric band near 1.93 μm. The feature at 1.85 μm is near the level of noise and thus it is difficult to determine if it is a real absorption feature. (f) Ratio spectrum of partially dehydrated Fe-sulfate from CRISM FRT 5814. The red marks indicate the beds in (d) over which the CRISM pixels were averaged. The signature is strongest in the bottom beds and decreases upward through the stratigraphic section where HiRISE images show increasing amounts of eolian debris covering the beds. (For interpretation of color mentioned in this figure the reader is referred to the web version of the article.)

branching lineations could result from erosion by the wind or disruption by crater ejecta and may not represent depositional structures like those seen in the Melas fans. The lack of a depositional basin at the site would argue against a fluvial origin, yet the planimetric pattern is consistent with terrestrial river-dominated deltas. The two alternative hypotheses presented do not address why the lineations appear to join with the main E–W trunk, unless that is just a coincidental association. A number of terrestrial studies have developed classification schemes for the planimetric pattern of the delta, which is dependent upon discharge regime, the sediment load of the river, the sediment grain size, water depth and the relative magnitudes of tides, waves and currents (Galloway, 1975; Coleman and Wright, 1975; Orton and Reading, 1993; Reading and Collinson, 1996). The overall digitate nature and wide-spreading angles of the distributary channels are characteristics of river-dominated deltas. The deltaic depositional pattern is consistent with a river that transported predominantly fine-grained material (Bhattacharya, 2006). The straight configuration of the distributary channels is consistent with formation on lower gradient slopes and relatively low discharge (Olariu and Bhattacharya, 2006). Additional ICs appear as sinuous lineations to the south of the LLD and appear to be residual deposits in which the surrounding material has been completely removed by the wind.

7.3. Ganges plateau light-toned materials

In addition to the LLD, there are numerous patches of light-toned material along the volcanic plains to the west of Ganges Chasma and a few outcrops along the floor of Ophir Cavus. Light-toned material seen on the floor of Ophir Cavus (Fig. 37a) does not exhibit bedding and is morphologically distinct from both the LLD and the light-toned material on the lava plains. The

Fig. 32. CTX mosaic (not geometrically corrected) of the Ganges plateau LLD, Allegheny Vallis, and the pit Ophir Cavus. The LLD is mapped in purple. The main branches of Allegheny Vallis are shown in dark blue while less prominent branches are shown in light blue. Locations of HiRISE images are shown by white boxes. Yellow boxes indicate locations of later figures. A degraded crater (DC) with light-toned ejecta is also noted. Illumination is from the left. (For interpretation of color mentioned in this figure the reader is referred to the web version of the article.)

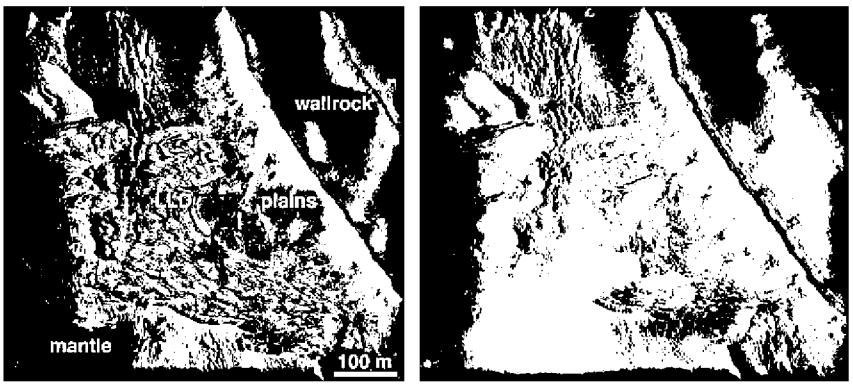

Fig. 33. Stratigraphy along the edge of Ganges Chasma illustrating the wallrock composed of volcanic plains materials and the LLD above. A darker-toned eolian mantle obscures most of the LLD. Portion of HiRISE RGB image PSP_5939_1720 (left) and stereo anaglyph (right). Illumination is from the left. (For interpretation of color mentioned in this figure the reader is referred to the web version of the article.)

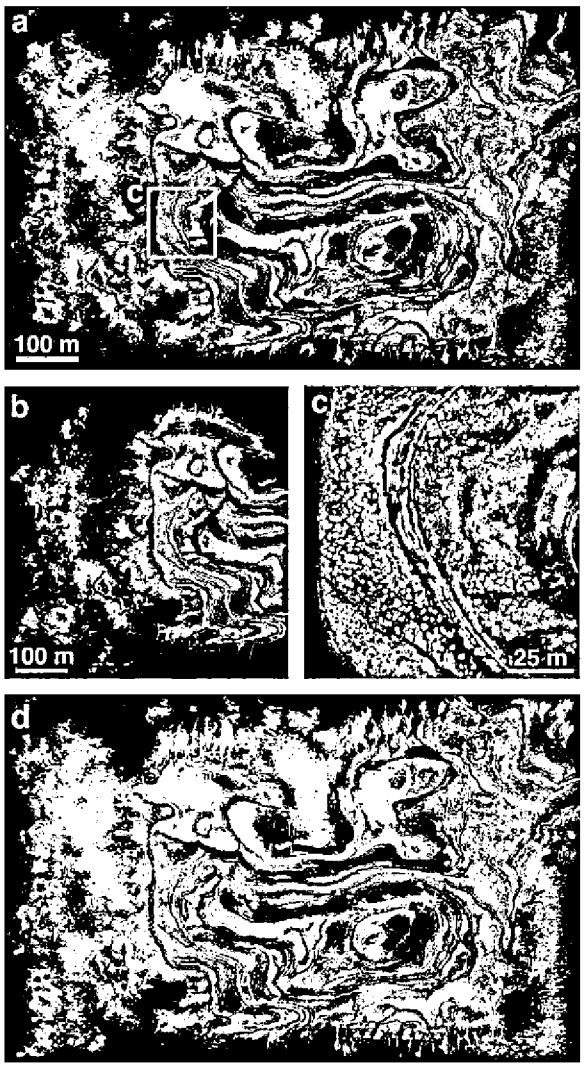

Fig. 34. (a) Example of different beds within the LLD near Ganges. Location of blowup shown by yellow box. Portion of HiRISE image PSP_5161_1720. Illumination is from the left. (b) RGB image reveals color variations in the beds typical of the LLDs. (c) Blowup demonstrating the different scales of polygonal fracturing along the light-toned beds. (d) HiRISE stereo anaglyph of the same region shown in (a). (For interpretation of color mentioned in this figure the reader is referred to the web version of the article.)

light-toned unit on the floor of Ophir Cavus could be older material exposed by the formation of the pit, or it could represent water-lain material associated with the formation of the channels that emanate from the pit.

The largest light-toned patches are located along the ejecta of a degraded crater (Fig. 32, DC), just to the north of Ophir Cavus. The light-toned patches can exhibit cracking and polygonal fractures (Fig. 37b). Similar light-toned materials are also exposed along the lava plains southwest of the Juventae plains LLD (HiRISE image PSP_006836_1750), by the lava plains in and around the Candor LLD, and south of Eos Chasma, suggesting it may be a common surface feature on the Valles Marineris plateau. In some cases, such as the lava plains south of Eos, these light-toned deposits are not associated with LLDs and are found in Noachian-aged terrains, implying they were deposited prior to the LLDs and may represent Noachian alteration. Stereo image pairs show that the light-toned material on the lava plains is commonly on surfaces adjacent to but topographically higher than the channels (Fig. 37c and d). There is no evidence for light-toned material within the channels, although eolian debris and ripples cover the channel floors.

7.4. CRISM results for the Ganges plateau LLD

As shown in Fig. 38, the small exposures of LLD near Ganges appear bluish-green in CRISM false-color RGB images, similar to the other four sites described previously. The largest and brightest exposures are found directly adjacent to the western edge of the chasma and exhibit spectral signatures indicative of opal (Fig. 38c and d). The opal-bearing unit is often the lowest stratigraphic layer in the LLD exposures (Le Deit et al., 2008b, 2009), although this may be in part an artifact of the difference in areal exposure between this bottom layer and the steep scarps associated with the overlying beds. In addition, the opal-bearing unit can exhibit small ridges that intersect at high angles (Fig. 38c). The overlying materials are spectrally similar to dusty regions, consistent with the HiRISE and CTX images that show the region to be mantled by eolian debris or a partially lithified dark unit (e.g., Fig. 33). We have not yet detected sulfates or other hydrated phases associated with the plateau LLD in this location.

8. Discussion

As discussed by Weitz et al. (2008), proposed origins for the VM plateaus LLDs include eolian, fluvio-lacustrine, and pyroclastic volcanism. The identification of valleys or channels at all five LLD locations, inverted channels at three of the deposits, and spectral evidence for aqueous minerals provides compelling evidence for a fluvial-lacustrine origin or perhaps aqueous reworking of sediments deposited by another process. CRISM spectra acquired at all of the sites discussed here are consistent with the presence of opaline silica, and the LLDs south of Melas and west of Juventae show evidence for Fe-sulfates (Milliken et al., 2008). Opal-bearing materials are found on the upper surfaces of the lava plains or at the base of the LLDs, but not within the light-toned layered beds. The type of jarosite detected at the Melas location is also indicative of low-temperature acidic fluids and does not require high temperatures (e.g., hydrothermal processes) to form. The mineralogy at all five VM plateaus LLDs locations supports low-temperature alteration or precipitation of minerals out of evaporating fluids as a result of the chemical weathering of basaltic lava flows, volcanic ash, and/or impact glass (Milliken et al., 2008). The presence of Fe-sulfates near Juventae and Melas suggest these deposits were formed by or interacted with acidic fluids with pH < 4. Based on the solubility of amorphous silica, fluids at the other sites likely represent pH < 9 (Milliken et al., 2008), but the specific aqueous geochemistry will remain ambiguous until a full alteration assemblage can be identified.

8.1. Comparison to other equatorial LLDs

In order to further investigate a fluvio-lacustrine origin, we have compared the VM plateaus LLDs to light-toned layering seen at nine other equatorial locations on Mars where HiRISE images have been acquired (Fig. 39). Strata in Holden Crater are interpreted as sediments deposited by aqueous activity (Grant et al., 2008). These light-toned units exhibit meter-scale layering and some color differences between individual beds (Fig. 39a), but they are relatively more uniform and lack the morphological variations when compared to the VM plateaus LLDs. The Eberswalde LLD represents sediments deposited in a fan delta (Malin and Edgett, 2003; Moore et al., 2003) and shares some similarities to the VM plateaus LLDs, including associated inverted channels, polygonal fracturing, as well as meter-scale layering that is eroding along distinct layer surfaces to produce cliff-bench patterns (Fig. 39b). However, the Eberswalde LLD has a narrow range of brightness and color differences, possibly because variations in composition, grain size, and

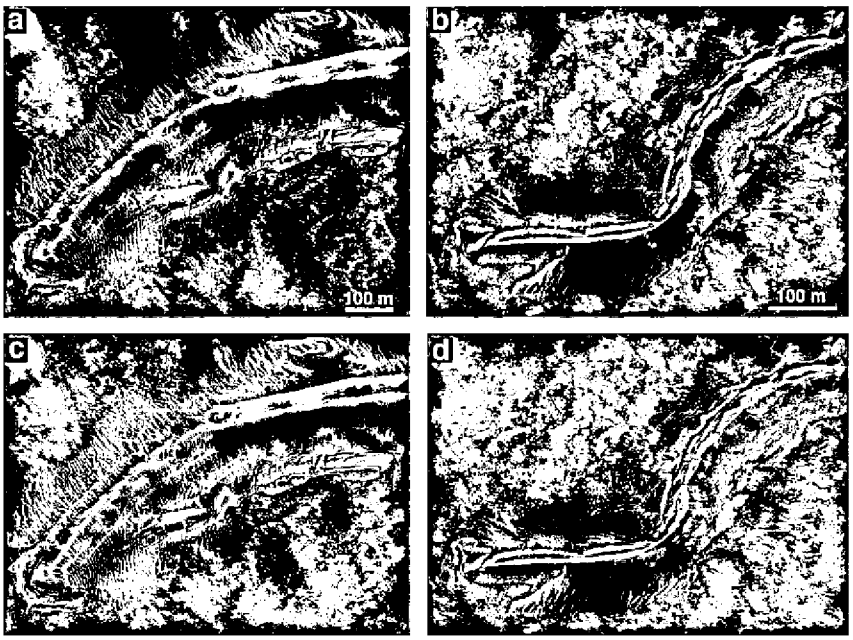

Fig. 35. (a and b) Examples of inverted channels seen in association with the Ganges plateau LLD. Light-toned layering can be seen within the ICs. Portion of HiRISE image PSP_5161_1720. Illumination is from the left. (c and d) Corresponding HiRISE stereo anaglyphs.

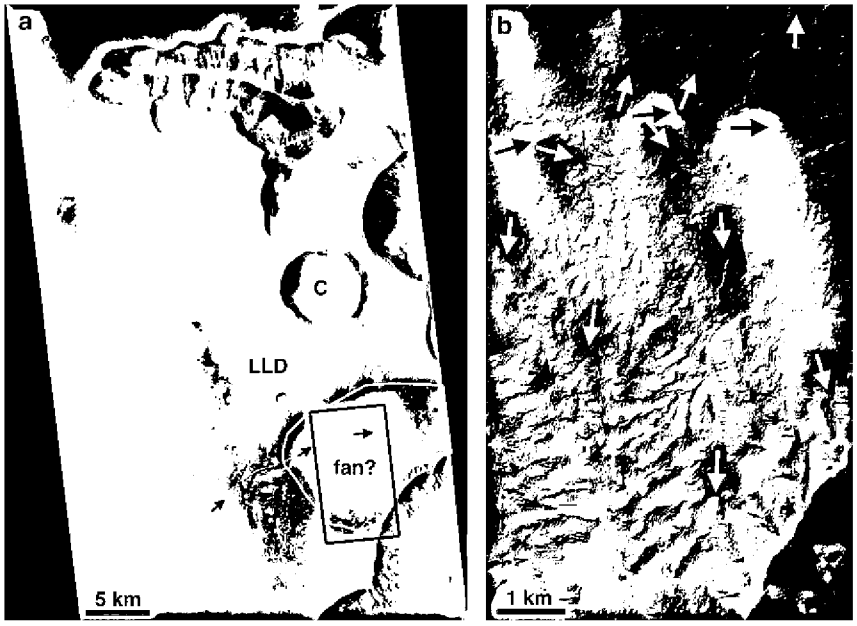

Fig. 36. (a) Portion of CTX image P11_5161_1715_XI_08S052W_070902 that shows the Ganges plateau LLD and a 5.5-km diameter crater, C, that disrupts it. An inverted channel (black arrows) can be mapped towards and within the LLD, and there is a possible depositional fan (white outline) that disperses out from the IC. Black box shows location of blowup (b) where lineations feather out from the IC (black arrows) in the north–south directions at high angles (white arrows). Arrows show inferred directions of water flow. Illumination is from the left.

cementation are less variable than in the VM plateaus LLDs. The Eberswalde deposit also contains boulders and many beds appear blocky, characteristics not observed in the VM plateaus LLDs.

Light-toned layered deposits with unknown or controversial origins include those inside Juventae Chasma, inside Gale crater, at Meridiani Planum, at Mawrth Vallis, and inside Becquerel crater (Fig. 39c–g). These deposits do not share many of the unique characteristics of the VM plateaus LLDs. Strata found in the Melas Chasma basin (Fig. 39h) likely represent sediments derived from the erosion of valleys along the walls in Melas and deposited in a paleolake (Quantin et al., 2005). As we discussed previously, these valleys probably formed at the same times as those found along the adjacent plateau in association with the Melas plateau LLD. The LLD in the Melas basin has the same cliff-bench morphology but lacks the color and brightness variations seen in the deposits along the plateau. However, obscuration by eolian debris may explain the absence of color and brightness heterogeneities in the Melas basin strata. Of these nine other Mars LLDs, only the Melas basin region has opal and jarosite (Metz et al., 2009) which could be genetically related to the same jarosite and opal seen on the plateau directly south.

Layered strata in channels at Ladon Valles appear morphologically to be the most similar to the VM plateaus LLDs (Fig. 39i).

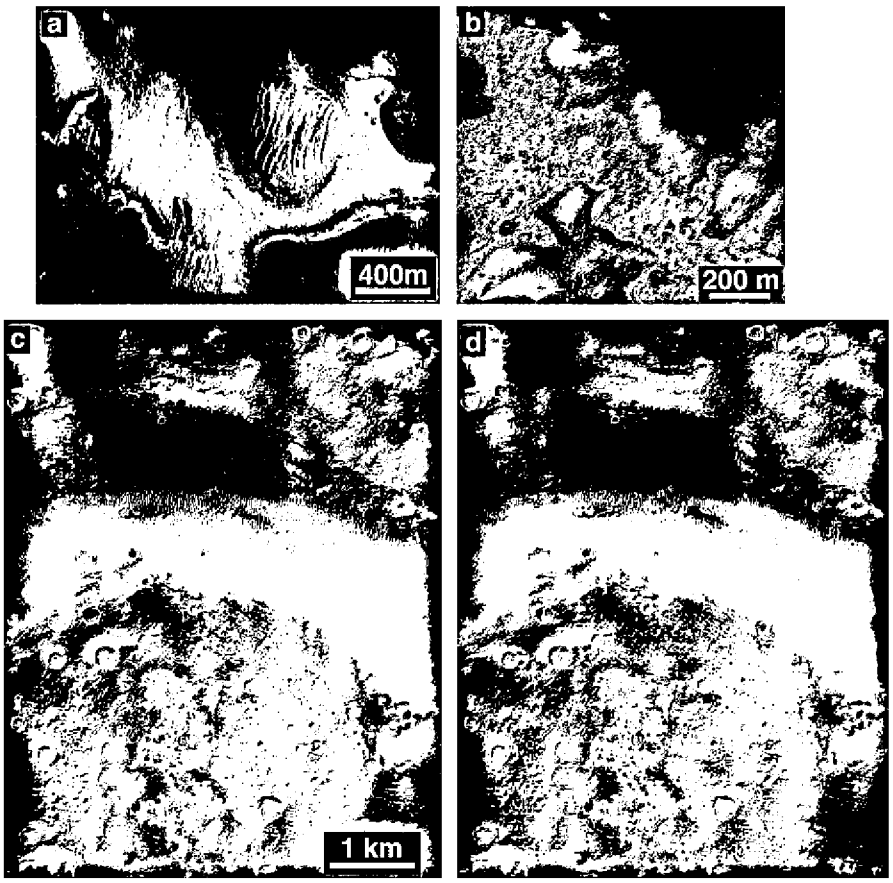

Fig. 37. Examples of light-toned materials along the Ganges plateau. (a) Light-toned material on the floor of Ophir Cavus does not resemble the LLD and could be evaporites or material deposited in association with water that partially filled the pit. Portion of HiRISE image PSP_5082_1700. Illumination is from the left. (b) Light-toned alteration along the lava plains just to the north of Ophir Cavus. Portion of HiRISE RGB image PSP_9934_1705. Illumination is from the left. (c) Light-toned material on the upper surfaces of the lava plains adjacent to Allegheny Vallis. (d) Stereo anaglyph of the same area shown in (c). Portion of HiRISE images PSP_8009_1715 and PSP_9578_1715. Illumination is from the left.

These light-toned layers exhibit color and brightness variations both between and within beds, as well as the cliff-bench erosional style similar to characteristics of the LLDs along the plateau. Ladon Valles contains several valleys that dissect the plains to the northeast of Holden and Eberswalde, potentially an extension downstream of Uzboi Vallis that breaches Holden crater (Grant and Parker, 2002). The light-toned layering is best observed in outcrops at the terminal portions of the valleys.

Although we group all five VM plateaus LLDs as the same mapped unit, there are subtle differences in the morphology and composition between the five deposits that suggest unique depositional histories for each region. For example, inverted channels are only found at Juventae, Ius, and Ganges LLDs. The extent of cliff-bench morphologies for any given LLD may be a reflection of the amount of wind erosion at the sites or variations in the degree of cementation between beds. In any case, these five deposits share more similarities than disparities relative to other light-toned deposits on Mars, supporting a similar origin in comparable environments.

8.2. Interactions with water

The color and brightness differences between layers in the strata of the VM plateaus LLDs could reflect distinct materials deposited and/or altered by water. For example, the darker-toned beds could be material derived from the erosion of the darker-toned lava plains. The lighter-toned beds could be reworked plains material that has been chemically altered by interaction with water or late-stage evaporates after the water sublimated. The slight variations in CRISM spectral signatures observed for the Juventae LLD suggest that multiple related phases might be present (Bishop et al., 2009). However, without knowing the amount of unaltered material that is still present, it is impossible to determine if the alteration was complete and what may have been the precursor material(s). Because CRISM has not detected any phyllosilicates in association with the LLDs and ICs, the water may not have interacted for long periods of time with the sediments or the pH conditions may have been unfavorable for clay formation (Bibring et al., 2006). Regardless, the identification of opaline silica, and, in some cases sulfates, requires water to be present long enough to alter the rocks or sediments (Milliken et al., 2008). In addition, the observation that Fe-sulfates are found stratigraphically above beds containing opaline silica is consistent with evaporation sequences in acidic waters produced by dissolution of a basaltic precursor (Milliken et al., 2008). While we can state that the opal and Fe-sulfates are consistent with alteration of basaltic compositions at low water-to-rock ratios, we cannot exclude the possibility that the fluids that precipitated these phases actually altered rock from some other place and then flowed to these regions. In this scenario, the unaltered material in the VM plateaus LLDs may have no direct link to the composition of the altered phases (the opal and Fe-sulfates). In situ data is needed to distinguish between these scenarios.

8.3. Timing of LLD emplacement

The formation time of the VM plateau LLDs can be constrained from stratigraphic relationships. The LLDs are strati-

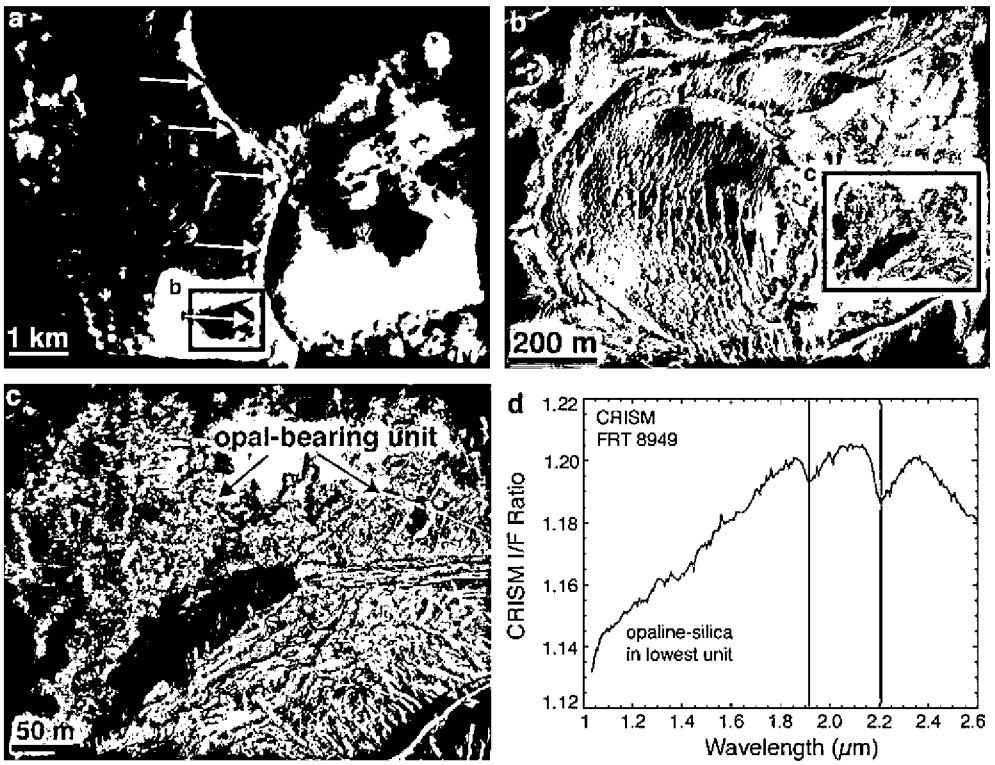

Fig. 38. (a) Close-up of CRISM FRT 8949 showing that the small exposures of LLD appear green (white arrows). Illumination is from the left. (b) HiRISE false-color close-up of an eroded crater (black box in a) showing the small outcrops of LLD. HiRISE image PSP_005939_1720. Illumination is from the left. (c) HiRISE close-up (black box in b) showing the opal-bearing LLD outcrops in detail. The opal is found at the base of the LLD in units that exhibit raised ridges, possibly filled fractures. The thicker overlying beds are too dusty to obtain clear spectral signatures of hydrated materials. (d) CRISM spectral ratio creating by averaging pixels from the unit marked by white arrows in (a). Similar to other deposits, the greenish units in CRISM images are consistent with opal. (For interpretation of color mentioned in this figure the reader is referred to the web version of the article.)

graphically above volcanic plains on the plateaus interpreted to be Early Hesperian in age (McCauley, 1978; Whitbeck et al., 1991; Scott and Tanaka, 1986). The Valles Marineris trough system is believed to have started to open in the Early Hesperian and continued into the Late-Hesperian (Tanaka, 1986; Lucchitta and 9 colleagues, 1992). Because we observe valleys along the walls of Melas and Juventae Chasmata that are within tens of kilometers of LLDs and valleys on these two plateaus, some of the LLDs must have been emplaced after formation of the chasmata. However, continued extension and backwasting along portions of the chasmata could have destroyed the LLDs along the plateaus. For example, erosion and collapse along the southeastern end of Allegheny Vallis has created a small tributary canyon that extends out from Ganges Chasma (Harrison and Grimm, 2005). If Allegheny Vallis is the source of sediment for the Ganges plateau LLD then expansion of Ganges Chasma may have also destroyed some of the LLD at this location. Formation of the tributary canyons by sapping probably removed portions of the LLD along the plateau adjacent to Ius Chasma. The absence of any LLD inside these tributary canyons would support this interpretation. Thus, we can propose that the VM plateau LLDs were most likely emplaced in the Middle- to Late-Hesperian after most of the chasmata had formed but while localized backwasting was still occurring along some wallrock.

8.4. Associated fluvial landforms

The fluvial landforms differ depending upon which LLD they occur. Most of the fluvial landforms associated with the Juventae plateau LLD are inverted channels whereas Melas and Candor are dominated by negative relief valleys. In the case of Juventae and Ganges Chasmata, light-toned beds can be identified within inverted channels, providing compelling evidence in support of a fluvial-lacustrine origin for these two LLDs. In contrast, valleys found on the plateaus of Melas and Candor incise the LLD and may have formed by later surface runoff that affected but did not emplace the layered deposits. For example, the LLDs on the plateaus of Melas and Candor could be pyroclastic deposits where precipitation carved valleys in the ash that are preserved because of the friable nature relative to the adjacent and more resistant lava plains. At Ius, the valleys are filled with layered material and also incise the LLD so multiple episodes of fluvial activity and erosion were likely. Nevertheless, the observation that all five LLDs exhibit fluvial landforms indicates some hydrological activity at these locations, even though we cannot directly link fluvial activity to the emplacement of all the LLDs.

The concentration of former streams and associated sediments along the Valles Marineris plateaus at these five locations might be due to local precipitation resulting from local climatic effects, and/or to regional heatflow that triggered snowmelt in specific regions (Mangold et al., 2008). Much or all of this precipitation could have resulted from Hesperian volcanic activity at Tharsis and volatiles released from circum-Chryse outflow channel flooding (Baker et al., 1991; Harrison and Grimm, 2004). The source of water and sediment remains uncertain, however, in part because the full extent of the valley systems is unknown. Backwasting of the canyon walls is likely, but the extent cannot be constrained. Backwasting presumably destroyed portions of the watersheds and some valleys likely remain buried beneath eolian debris on the lava plains farther from the chasmata walls. With the exception of Ganges, there is no evidence for a large-scale watershed for these systems and the scale of the drainage does not imply

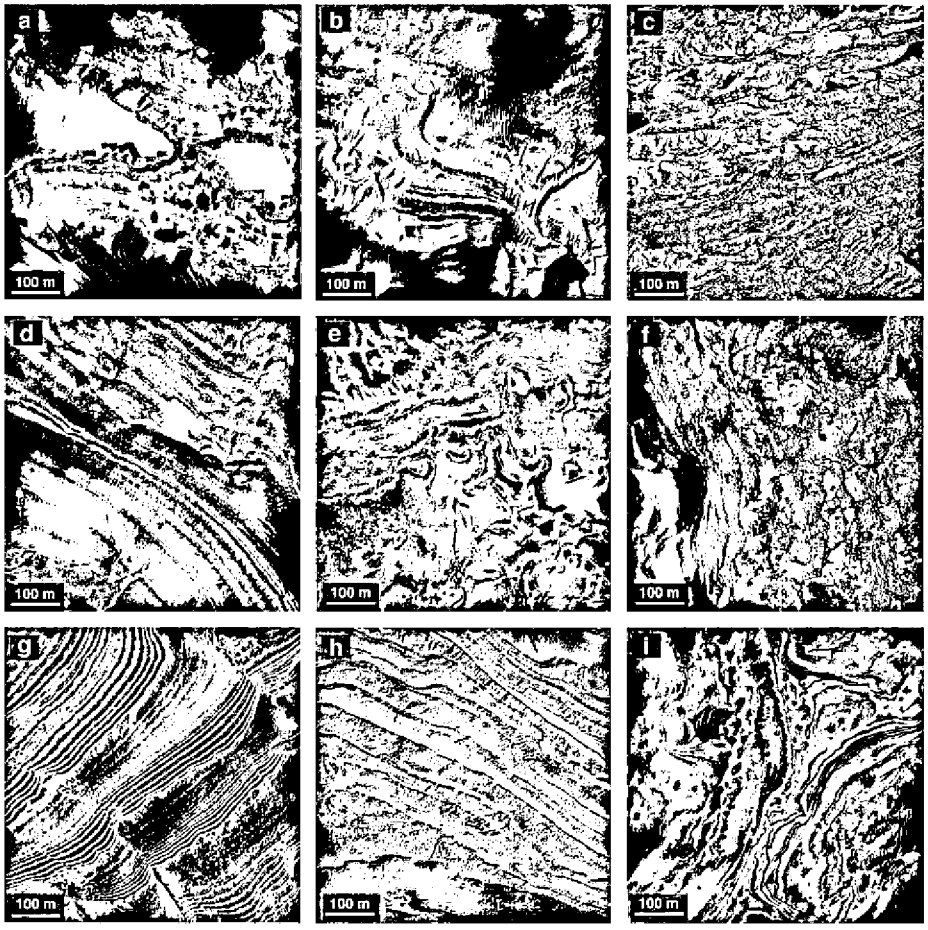

Fig. 39. Different false-color images of LLDs found on Mars. (a) Holden Crater. HiRISE image PSP_004211_1525. (b) Eberswalde Delta. HiRISE image PSP_1534_1560. (c) ILD of Juventae Chasma. HiRISE image PSP_005557_1755. (d) Gale Crater. HiRISE image PSP_007501_1750. (e) Meridiani Planum. HiRISE image PSP_007440_1845. (f) Mawrth Vallis. HiRISE image PSP_001929_2050. (g) Becquerel Crater. HiRISE image PSP_001918_1735. (h) Melas Chasma paleolake basin. HiRISE image PSP_007667_1700. (i) Ladon Vallis. HiRISE image PSP_006637_1590. The deposits that share the most characteristics with the Valles Marineris plateaus LLDs are those found in Ladon Vallis. Illumination is from the left for all images.

that an extensive or rugged upstream section once existed and has been removed.

The planimetric pattern of terrestrial alluvial streams has been well studied, with three major types initially identified related to increases in flow intensity: straight, meandering and braided (multiple flowpaths at low flow) (Leopold and Wolman, 1957, 1960). Thresholds occur between the three types, in the order listed, as valley gradient and dominant discharge increase. In addition, the cohesiveness of the banks, resulting from clay-rich sediment, cementation, or vegetation, is a factor in channel pattern (Ferguson, 1987). Streams that develop in strongly cohesive materials with low flow typically are straight in planform because the competency inhibits systematic bank erosion (Schumm, 1960, 1963, 1968; Ferguson, 1973). The channel/valley planimetric patterns seen in association with the VM plateaus LLDs generally have straight configurations, presumably reflecting a cohesive substrate with low gradient. The THEMIS IR images of the LLDs, which can be used to infer sizes of particles, differ in their brightness depending upon the properties of the adjacent terrains. Furthermore, a dark mantle obscures much of the deposits which complicates interpretation of the particle sizes from THEMIS IR data. Nevertheless, particle sizes in the source material were most likely small, perhaps sub-pebble, and there is an abundance of fine-grained particles on Mars redistributed by eolian processes. The most probable sediment source for the LLDs could have been reworked eolian or pyroclastic material that was cemented.

9. Conclusions

Our analysis of light-toned layered deposits on the plateaus surrounding Valles Marineris using new Mars Reconnaissance Orbiter data reveals that the equatorial regions may have remained wet for a much longer duration than previously noted. The VM plateaus LLDs are distinct in lithology and composition from ILDs within the canyon system, suggesting the materials and deposition processes occurring on the plateaus of Valles Marineris were distinct from those within the chasmata. The opaline and Fe-sulfate mineralogy of several of the beds within and at the base of the LLDs is consistent with low-temperature acidic aqueous alteration of basaltic materials. The opal and Fe-sulfates could simply be pore-filling cements that came after the sediments were laid down. Alternatively, they could have been precipitated out of the fluid that also transported the sediments if the processes were contemporaneous. Without in situ data from a rover to examine textural information, we cannot distinguish between these two scenarios.

All five VM plateaus LLDs have associated valley or channel systems and three of the deposits have associated inverted channels, providing compelling support for a fluvial origin of the light-toned strata. Valleys along the walls of Melas and Juventae Chasmata post-date formation of the chasmata and most likely formed contemporaneous to aqueous activity that occurred on the adjacent plateaus. The identification of valley networks and likely associ-

ated fluvial sediments indicates that precipitation and surface runoff must have occurred for sustained periods in the Hesperian around Valles Marineris, suggesting an active hydrological cycle beyond the Noachian in this region.

Acknowledgments

We are grateful to the HiRISE, CTX, and CRISM teams for collection of the data used in this study. We thank F. Chuang for assistance with MOLA PEDR data. M. Rosiek, S. Wilson Purdy, and J. Griffes provided assistance with the HiRISE DEM data. We appreciate comments from V. Gulick, K. Herkenhoff and reviews by B. Ehlmann and J. Rice. This manuscript is PSI Contribution 454.

References

Baker, V.R., Strom, R.G., Gulick, V.C., Kargel, J.S., Komatsu, G., Kale, V.S., 1991. Ancient oceans, ice sheets and the hydrological cycle on Mars. Nature 352, 589–594.

Beyer, R.A., McEwen, A.S., 2005. Layering stratigraphy of eastern Coprates and northern Capri Chasmata, Mars. Icarus 179, 1–23. doi:10.1016/j.icarus.2005.06.014.

Bhattacharya, J.P., 2006. Deltas. In: Walker, R.G., Posamentier, H. (Eds.), Facies Models Revisited, vol. 84. SEPM Special Publication, pp. 237–292.

Bibring, J.P., Langevin, Y., Mustard, J.F., Poulet, F., Arvidson, R., Gendrin, A., Gondet, B., Mangold, N., Pinet, P., Forget, F., the OMEGA Team, 2006. Global mineralogical and aqueous Mars history derived from OMEGA Mars Express Data. Science 312, 400–404.

Bishop, J.L., Parente, M., Weitz, C.M., Noe Dobrea, E.Z., Roach, L.A., Murchie, S.L., McGuire, P.C., McKeown, N.K., Brown, A.J., Calvin, W.M., Milliken, R.E., Mustard, J.F., 2009. Mineralogy of Juventae Chasma: Sulfates in the light-toned mounds, mafic minerals in the bedrock, and hydrated silica and hydroxylated ferric sulfate on the plateau. J. Geophys. Res., submitted for publication.

Cabrol, N.A., Grin, E.A., 2001. The evolution of lacustrine environments on early Mars: Is Mars only hydrologically dormant? Icarus 149, 291–328.

Carr, M., 1995. The martian drainage system and the origin of valley networks and fretted channels. J. Geophys. Res. 100, 7479–7507.

Carr, M., Malin, M.C., 2000. Meter-scale characteristics of martian channels and valleys. Icarus 146, 366–386.

Catling, D.C., Wood, S.E., Leovy, C., Montgomery, D.R., Greenberg, H.M., Glein, C.R., Moore, J.M., 2006. Light-toned layered deposits in Juventae Chasma, Mars. Icarus 181, 26–51.

Chapman, M.G., Tanaka, K.L., 2001. Interior trough deposits on Mars: Subice volcanoes? J. Geophys. Res. 106 (E5), 10087–10100.

Coleman, J., Wright, L., 1975. In: Broussard, M. (Ed.), Modern River Deltas: Variability of Processes and Sand Bodies. Houston Geol. Soc., Houston, TX, pp. 99–149.

Coleman, N.M., Dinwiddie, C.L., Casteel, K., 2007. High outflow channels on Mars indicate Hesperian recharge at low latitudes and the presence of Canyon Lakes. Icarus 189, 344–361.

Craddock, R.A., Howard, A.D., 2002. The case for rainfall on a warm, wet early Mars. J. Geophys. Res. 107 (E11), 5111. doi:10.1029/2001JE001505.

Edgett, K.S., 2005. The sedimentary rocks of Sinus Meridiani: Five key observations from data acquired by the Mars Global Surveyor and Mars Odyssey orbiters. Mars 1, 5–58. doi:10.1555/mars.2005.0002.

Edgett, K.S., Malin, M.C., 2003. The layered upper crust of Mars: An update on MGS MOC observations after two Mars years in the mapping orbit. Lunar Planet. Sci. XXXIV. Abstract 1124, Lunar and Planetary Institute, Houston, TX.

Edgett, K.S., Malin, M.C., 2004. The geologic record of early Mars: A layered, cratered, and "valley-ed" volume. Lunar Planet. Sci. XXXV. Abstract 1188, Lunar and Planetary Institute, Houston, TX.

Ferguson, R.I., 1973. Channel pattern and sediment type. Area 5, 38–41.

Ferguson, R.I., 1987. Hydraulic and sedimentary controls of channel pattern. In: Richards, K.S. (Ed.), River Channels: Environment and Process. Blackwell, Oxford, pp. 129–158.

Galloway, W.E., 1975. Process framework for describing the morphologic and stratigraphic evolution of deltaic depositional systems. In: Broussard, M.L. (Ed.), Deltas, Models for Exploration. Houston Geological Society, Houston, TX, pp. 87–98.

Goryniuk, M.C., Rivard, B.A., Jones, B., 2004. The reflectance spectra of opal-A (0.5–25 μm) from the Taupo Volcanic Zone: Spectra that may identify hydrothermal systems on planetary surfaces. Geophys. Res. Lett. 31. L24701. doi:10.1029/2004GL021481.

Grant, J.A., 1987. The geomorphic evolution of eastern Margaritifer Sinus, Mars. In: Advances in Planetary Geology, NASA Tech. Memo., NASA TM-89871, pp. 1–268.

Grant, J.A., Parker, T.J., 2002. Drainage evolution of the Margaritifer Sinus Region, Mars. J. Geophys. Res. 107. doi:10.1029/2001JE001678.

Grant, J.A., Irwin III, R.P., Grotzinger, J.P., Milliken, R.E., Tornabene, L.L., McEwen, A.S., Weitz, C.M., Squyres, S.W., Glotch, T.D., Thomson, B.J., 2008. HiRISE imaging of impact megabreccia and sub-meter aqueous strata in Holden Crater, Mars. Geology 36, 195–198.

Gulick, V.C., 2001. Origin of the valley networks on Mars: A hydrological perspective. Geomorphology 37, 241–268.

Harrison, K.P., Grimm, R.E., 2004. Tharsis recharge: A source of groundwater for martian outflow channels. Geophys. Res. Lett. 31. L14703. doi:10.1029/2004GL020502.

Harrison, K.P., Grimm, R.E., 2005. Groundwater-controlled valley networks and the decline of surface runoff on early Mars. J. Geophys. Res., 110. doi:10.1029/2005JE002455.

Hynek, B.M., Phillips, R.J., Arvidson, R.E., 2003. Explosive volcanism in the Tharsis region: Global evidence in the martian geologic record. J. Geophys. Res. 108 (E9), 5111. doi:10.1029/2003JE002062.

Irwin III, R.P., Howard, A.D., 2002. Drainage basin evolution in Noachian Terra Cimmeria, Mars. J. Geophys. Res. 107 (E7), 5056. doi:10.1029/2001JE001818.

Kirk, R.L.18 colleagues, 2008. Ultrahigh resolution topographic mapping of Mars with MRO HiRISE stereo images: Meter-scale slopes of candidate Phoenix landing sites. J. Geophys. Res. 113, E00A24. doi:10.1029/2007JE003000.

Kochel, R.C., Piper, J., 1986. Morphology of large valleys on Hawaii: Evidence for groundwater sapping and comparisons with martian valleys. Proc. Lunar Planet. Sci. Conf. 17th, Part 1, J. Geophys. Res. 91 (Suppl.), E175–E192.

Komatsu, G., Geissler, P.E., Strom, R.G., Singer, R.B., 1993. Stratigraphy and erosional landforms of layered deposits in Valles Marineris, Mars. J. Geophys. Res. 98 (E6), 11105–11121.

Le Deit, L., Bourgeois, O., Le Mouelic, S., Mege, D., Combe, J.P., Sotin, C., Masse, M., 2008a. Light-toned layers on plateaus above Valles Marineris (Mars). Lunar Planet. Sci. XXXIX. Abstract 1740, Lunar and Planetary Institute, Houston, TX.

Le Deit, L., Le Mouelic, S., Bourgeois, O., Mege, D., Masse, M., Quantin-Nataf, C., Sotin, C., Bibring, J.-P., Gondet, B., and Langevin, Y., 2008b. Composition and morphology of hydrated layered deposits on the plains around Valles Marineris (Mars). Workshop on Martian Phyllosilicates. Abstract 7016, CNES, Paris, France.

Le Deit, L., Bourgeois, O., Mege, D., Le Mouelic, S., Masse, M., Hauber, E., Jaumann, R., Bibring, J.-P., 2009. Geological history of a light-toned formation draping the plateaus in the region of Valles Marineris, Mars. Lunar Planet. Sci. XL. Abstract 1856, Lunar and Planetary Institute, Houston, TX.

Leopold, L.B., Wolman, M.G., 1957. River channel patterns: Braided, meandering, and straight, pp. Professional Paper 282-B, US Geological Survey, Reston.

Leopold, L.B., Wolman, M.G., 1960. River meanders. Geol. Soc. Am. Bull. 71 (6), 769–793.

Lewis, K.W., Aharonson, O., Grotzinger, J.P., Kirk, R.L., McEwen, A.S., Suer, T.-A., 2008. Quasi-periodic layering in the sedimentary rock record of Mars. J. Geophys. Res., submitted for publication.

Lucchitta, B.K., 1990. Young volcanic deposits in the Valles Marineris, Mars?. Icarus 86, 476–509.

Lucchitta, B.K., 2005. Light layer and sinuous ridges on plateau near Juventae Chasma, Mars. Lunar Planet. Sci. XXXVI. Abstract 1500, Lunar and Planetary Institute, Houston, TX.

Lucchitta, B.K., and 9 colleagues, 1992. The canyon system on Mars. In: Kieffer, H.H., Jakosky, B.M., Snyder, C.W., Matthews, M.I. (Eds.), Mars. University of Arizona Press, Tucson, pp. 453–492.

Lucchitta, B.K., Isbell, N.K., Howington-Kraus, A., 1994. Topography of Valles Marineris: Implications for erosional and structural history. J. Geophys. Res. 99 (E2), 3783–3798.

Malin, M.C., Edgett, K.S., 2000. Sedimentary rocks of early Mars. Science 290, 1927–1937.

Malin, M.C., Edgett, K.S., 2001. Mars Global Surveyor Mars Orbiter Camera: Interplanetary cruise through primary mission. J. Geophys. Res. 106 (E10), 23429–23570.

Malin, M.C., Edgett, K.S., 2003. Evidence for persistent flow and aqueous sedimentation on early Mars. Science 302, 1931–1934.

Malin, M.C., Bell III, J.F., Cantor, B.A., Caplinger, M.A., Calvin, W.M., Clancy, R.T., Edgett, K.S., Edwards, L., Haberle, R.M., James, P.B., Lee, S.W., Ravine, M.A., Thomas, P.C., Wolff, M.J., 2007. Context Camera Investigation on board the Mars Reconnaissance Orbiter. J. Geophys. Res. 112. E05S04. doi:10.1029/2006JE002808.

Mangold, N., Qunatin, C., Ansan, V., Delacourt, C., Allemand, P., 2004. Evidence for precipitation on Mars from dendritic valleys in the Valles Marineris area. Science 305, 78–81.

Mangold, N., Ansan, V., Masson, P., Quantin, C., Neukum, G., 2008. Geomorphic study of fluvial landforms on the northern Valles Marineris plateau, Mars. J. Geophys. Res. 113. E08009. doi:10.1029/2007JE002985.

McCauley, J.F., 1978. Geologic map of the Coprates Quadrangle of Mars, scale 1:5,000,000. US Geol. Surv. Misc. Inv. Series Map I-897.

McEwen, A.S., Malin, M.C., Carr, M.H., Hartmann, W.K., 1999. Voluminous volcanism on early Mars revealed in Valles Marineris. Nature 397, 584–586.

McEwen, A.S., and 14 colleagues, 2007. Mars Reconnaissance Orbiter's High Resolution Imaging Science Experiment (HiRISE). J. Geophys. Res. 112. E05S02. doi:10.1029/2005JE002605.

McEwen, A.S., and 69 colleagues, 2009. The High Resolution Imaging Science Experiment (HiRISE) during MRO's Primary Science Phase (PSP). Icarus, in this issue, doi:10.1016/j.icarus.2009.04.023.

Metz, J., Grotzinger, J., Mohrig, D., Prather, B., Pirmez, C., Milliken, R., McEwen, A., Weitz, C., 2009. Sublacustrine depositional fans in southwest Melas Chasma. J. Geophys. Res., submitted for publication.

Milliken, R.E., Mustard, J.F., 2005. Quantifying absolute water content of minerals using near-infrared reflectance spectroscopy. J. Geophys. Res. 110 (E12). doi:10.1029/2005JE002534.

Milliken, R.E., Swayze, G., Arvidson, R., Bishop, J., Clark, R., Ehlmann, B., Green, R., Grotzinger, J., Morris, R., Murchie, S., Mustard, J., Weitz, C., 2008. Opaline silica in young deposits on Mars. Geology 36, 847–850.

Moore, J.M., Howard, A.D., Dietrich, W.E., Schenk, P.M., 2003. Martian layered fluvial deposits: Implications for Noachian climate scenarios. Geophys. Res. Lett. 30 (24), 2292. doi:10.1029/2003GL019002.

Murchie, S., and 49 colleagues, 2007. Compact Reconnaissance Imaging Spectrometer for Mars (CRISM) on Mars Reconnaissance Orbiter (MRO). J. Geophys. Res. 112. E05S03. doi:10.1029/2006JE002682.

Murchie, S., Roach, L., Seelos, F., Milliken, R., Mustard, J., Arvidson, R., Wiseman, S., Lichtenberg, K., Andrews-Hanna, J., Bishop, J., Bribing, J.P., Parente, M., Morris, R., 2009. Compositional evidence for the origin of layered deposits in Valles Marineris, Mars. J. Geophys. Res., submitted for publication.

Mustard, J.F., Murchie, S.L., Pelkey, S.M., Ehlmann, B.L., Milliken, R.E., Grant, J.A., Bibring, J.-P., Poulet, F., Bishop, J., Roach, L., Seelos, F., Humm, D.the CRISM Science Team, 2008. Hydrated silicate minerals on Mars observed by the CRISM instrument on MRO. Nature 454, 305–309.

Nedell, S.S., Squyres, S.W., Andersen, D.W., 1987. Origin and evolution of the layered deposits in the Valles Marineris, Mars. Icarus 70, 409–441.

Okubo, C.H., Lewis, K.W., McEwen, A.S., Kirk, R.L., 2009. Relative age of interior layered deposits in southwest Candor Chasma based on high-resolution structural mapping. J. Geophys. Res. 113. doi:10.1029/2008JE003181.

Olariu, C., Bhattacharya, J.P., 2006. Terminal distributary channels and delta front architecture of river-dominated delta systems. J. Sediment. Res. 76, 212–233, Perspectives. doi:10.2110/jsr.2006.026.

Orton, G., Reading, H.G., 1993. Variability of deltaic processes in terms of sediment supply, with particular emphasis on grain size. Sedimentology 40, 475–512.

Pain, C.F., Clarke, J.D.A., Thomas, M., 2007. Inversion of relief on Mars. Icarus 190 (2), 478–491. doi:10.1016/j.icarus.2007.03.017.

Pelkey, S.M., Mustard, J.F., Murchie, S., Clancy, R.T., Wolff, M., Smith, M., Milliken, R.E., Bibring, J.-P., Gendrin, A., Poulet, F., Langevin, Y., Gondet, B., 2007. CRISM multispectral summary products: Parameterizing mineral diversity on Mars from reflectance spectra. J. Geophys. Res. 112 (E8). doi:10.1029/2006JE002831.

Peterson, C., 1982. A secondary origin for the central plateau of Hebes Chasma. In: Merrill, R.B., Ridings, R. (Eds.), Proceedings of the 12th Lunar and Planetary Science Conference. Pergamon Press, New York and Oxford, pp. 1459–1471.

Quantin, C., Allemand, P., Mangold, N., Dromart, G., Delacourt, C., 2005. Fluvial and lacustrine activity on layered deposits in Melas Chasma, Valles Marineris, Mars. J. Geophys. Res. 110. doi:10.1029/2005JE002440.

Reading, H.G., Collinson, J.D., 1996. Clastic coasts. In: Reading, H.G. (Ed.), third ed., Sedimentary Environments: Processes, Facies and Stratigraphy Blackwell Science, Oxford, UK, pp. 154–231.

Roach, L.H., Mustard, J.F., Murchie, S.L., Bibring, J.-P., Forget, F., Lewis, K.W., Aharonson, O., Vincendon, M., Bishop, J.L., 2009. Testing evidence of recent hydration state change in sulfates on Mars. J. Geophys. Res., 114. doi:10.1029/2008JE003245.

Schumm, S.A., 1960. The shape of alluvial channels in relation to sediment type. US Geological Survey Professional Paper, P0352-B.

Schumm, S.A., 1963. Sinuosity of alluvial rivers on the Great Plains. Geol. Soc. Am. Bull. 74 (9), 1089–1099.

Schumm, S.A., 1968. River adjustment to altered hydrologic regimen; Murrumbidgee River and paleochannels, Australia. US Geological Survey, Reston, p. 65.

Scott, D.H., Tanaka, K.L., 1986. Geologic map of the western equatorial region of Mars. US Geol. Surv. Misc. Invest Ser., Map I-1802-A.

Spencer, J.R., Croft, S.K., 1986. Valles Marineris as karst: Feasibility and implications for martian atmospheric evolution. In: Carr, M., James, P., Conway, L., Pepin, R., Pollack, J. (Eds.), MECA Workshop on the Evolution of the martian Atmosphere. A Lunar and Planetary Institute Workshop held in Honolulu, Hawaii, August 9–10, 1985. LPI Technical Report 86-07. Lunar and Planetary Institute, Houston (CD-ROM).

Spencer, J.R., Fanale, F.P., 1990. New models for the origin of Valles Marineris closed depressions. J. Geophys. Res. 95, 14301–14313.

Tanaka, K.L., 1986. The stratigraphy of Mars. J. Geophys. Res. (Suppl. 91), E139–E158.

Weitz, C.M., McEwen, A.S., Okubo, C.H., Russell, P., Grant, J.A., Dundas, C., Bridges, N., the HiRISE Team, 2007. Early HiRISE observations of light-toned layered deposits. Lunar Planet. Sci. XXXVIII. Abstract 1442, Lunar and Planetary Institute, Houston (CD-ROM).

Weitz, C.M., Milliken, R.E., Grant, J.A., McEwen, A.S., Williams, R.M.E., Bishop, J.L., 2008. Light-toned strata and inverted channels adjacent to Juventae and Ganges chasmata, Mars. Geophys. Res. Lett. 35. L19202.

Whitbeck, N.E., Tanaka, K.L., Scott, D.H., 1991. Geologic map of the Valles Marineris region, Mars, United States Geological Survey Miscellaneous Investigations Series, Map I-2010, scale 1:2,000,000.

Williams, J., Paige, D.A., Manning, C.E., 2003. Layering in the wall rock of Valles Marineris: Intrusive and extrusive magmatism. Geophys. Res. Lett. 30 (12), 1623. doi:10.1029/2003GL017662.

Williams, R.E., Malin, M.C., Edgett, K.S., 2005. Remnants of the courses of fine-scale, precipitation-fed runoff streams preserved in the martian rock record. Lunar Planet. Sci. Conf. XXXVI. Abstract 1173.

Wray, J.J., Ehlmann, B.L., Squyres, S.W., Mustard, J.F., Kirk, R.L., 2008. Compositional stratigraphy of clay-bearing layered deposits at Mawrth Vallis, Mars. Geophys. Res. Lett. 35. L12202. doi:10.1029/2008GL034385.